Desalination and Water Treatment
www.deswater.com

doi: 10.5004/dwt.2023.30146

316 (2023) 44–70
December

Toward sustainable environmental cleanup: metal–organic frameworks in adsorption - a review

Bandar R. Alsehli

Department of Chemistry, Faculty of Science, Taibah University, Al-Madinah Al-Munawarah 30002, Saudi Arabia, Phone: +966-552-055-010; email: bshle@taibahu.edu.sa

Received 15 August 2023; Accepted 20 November 2023

ABSTRACT

Metal–organic frameworks (MOFs) have gained significant consideration as highly promising materials for adsorption and reducing environmental contamination. They exhibit unique catalytic chemistry and coordination capabilities, making them versatile in various applications such as catalysis, gas handling, drug delivery, sensing, and separation. Compared to traditional adsorbents, MOFs offer advantages like high adsorption potential, large surface area, tunable porosity, hierarchical structure, and recyclability. However, their low stability in water poses a challenge for real-world implementation. By carefully selecting metal ions and organic linkers, the efficiency and selectivity of MOFs can be controlled for the removal of specific contaminants. Researchers have identified thermally and water-stable MOFs and their composites with other materials for the removal of environmental pollutants in water, soil, and the atmosphere. This review critically discusses the efficiency of MOFs for adsorption and their mechanisms of action, as well as their potential in combination with other adsorbents. The growing body of research demonstrates the emerging value of MOFs in environmental applications and provides insights for the development of efficient treatment technologies for the removal of hazardous environmental emissions.

Keywords: Environmental pollution; Metal–organic frameworks; Adsorption; Porous materials; Isotherms

1. Introduction

The global risk of releasing toxic pollutants into the environment is increasing [1,2]. Every year, various hazardous materials, including NO/NO_2, SO_2/SO_3, CO/CO_2, organic nitrogen compounds (e.g., hydrogen cyanide), sulfur-containing compounds (e.g., organothiols), organic compounds, and different toxic metals, are discharged into water and air [3–6]. These toxic pollutants primarily result from human activities [7,8], such as the combustion of fossil fuels, the release of harmful industrial gases and vapors, chemical warfare agents, and the discharge of industrial effluents [9,10]. Releasing harmful gases/vapors, organic compounds, and various metals into the atmosphere and soil can cause significant harm to the environment and human health [11,12]. As a response to the escalating emissions of industrial gases/vapors, stringent regulations have been proposed to reduce maximum volatile organic compound (VOC) emissions within limits in EU Member States. Additionally, heavy metals pose serious environmental contamination issues due to their toxicity, persistence in natural conditions, and ability to enter the food chain. The contamination of soil and aquatic systems with heavy metals has become a challenging pollution problem due to their toxic effects, abundance, and bioaccumulation in the human body. Consequently, there is considerable interest and discussion around the effective elimination of toxic pollutants from the environment [5,9]. Currently, several environmental purification technologies exist, including ozonation, membrane separation, incineration, and electrochemical oxidation, to name a few [13–16].

However, most of these treatment methods are plagued by high costs, low efficiency, and the generation of secondary pollutants. In this context, adsorption is gaining prominence as an affordable advanced technology for environmental purification due to its cost-effectiveness, minimal by-product formation, ease of separation, and eco-friendliness. Furthermore, adsorption does not lead to the production of any harmful substances [17,18]. The adsorption of hazardous gases, toxic metals, and organic compounds relies on the adsorption capacity and selectivity of porous materials, whose specific structures can enable toxic substances to enter their pores and be trapped through van der Waals forces (physical adsorption) or chemical bonding between the adsorbent and adsorbate (chemical adsorption) [19–21]. The physical adsorption potential of a solid adsorbent is heavily influenced by its pore size, cavity, and specificity. Conversely, the chemical adsorption capability is closely tied to the porous (acidic or basic) functionality, atomic surface coordination, and electron density (electron-poor or electron-rich). The characterization of porous materials plays a crucial role in determining their properties, with the adsorption of guest molecules on solid surfaces being a critical factor. This adsorption process is governed not only by the interaction between guest molecules and the surfaces but also by the pore size and shape [22]. Numerous porous materials have been evaluated as adsorbents for physically adsorbing toxic compounds, possessing large and rigid/flexible structures. Examples include activated carbon, porous silica, aluminum silicate zeolites, carbon nanotubes, and resins, among others [23–25].

Inorganic or organic materials have traditionally been used over the past few decades for their porous properties. The most common porous materials are widely used, probably; activated carbon, which is often made by pyrolysis of high carbon materials. Despite the large areas and implicitly high adsorption capacities, the lack of ordered structures is the main disadvantage. Nevertheless, porous carbon materials have demonstrated their utility across a wide range of applications including, for example, the storage and separation of gases, the removal and recovery of solvents, or the treatment and purification of water [26]. Zeolites, in turn, represent a class of porous inorganic materials with highly ordered structures, the synthesis of which is normally carried out using an inorganic or organic form with strong interactions. If you remove the model, the infrastructure collapses. Zeolites also have a disadvantage in that the occasional use of simple elements such as aluminium, silicon and chalcogens does not encourage undue diversity. In spite of this aspect, zeolites have attained significant industrial usage in applications such as separation and catalysis [27,28].

A novel category of porous materials is emerging to address the limitations of the aforementioned materials by combining the characteristics of both organic and inorganic porous materials. Starting from the late 1990s, these materials, featuring an inorganic–organic hybrid network, have made a significant impact in the field of porous materials. This marked the inception of a new family of porous species known as porous coordination polymers (PCPs) or Metal–organic frameworks (MOFs). PCPs/MOFs exhibit well-defined pores ranging from micro- to mesopores, a large surface area, and a highly customizable framework with sizable, shapeable, and functionalizable pore surfaces [29–31]. The molecular structure of these frameworks is based on organic ligands serving as linkers and metal centers acting as connectors. The remarkable designability and functionality of the organic spacers, combined with the physical properties of the metal ions, allow for the creation of diverse functions within the frameworks, such as gas storage/adsorption, separation, catalysis, and other chemical or physical functionalities. The assembly of PCPs involves coordinative bonds and various types of interactions like noncovalent bonds (e.g., hydrogen bonds, π-electron stacking, or van der Waals interactions), which contribute to the structural flexibility and dynamics in the crystalline state, further enhancing the unique nature of PCPs among porous materials. With advancements in synthetic techniques and accumulated knowledge over the past decade, chemists are now equipped to design innovative porous materials by harnessing the full potential of the chemical components and architectural topologies [32–35]. Due to their unparalleled inner surface area, straightforward chemical control, and exceptional capacity to selectively adsorb large quantities of guest species, this class of porous materials quickly rose to prominence in the field of materials science [36]. The potential of MOFs in addressing environmental pollution lies in their ability to easily decorate the high density of adsorption sites within their internal surfaces through post-synthetic modifications [37–39].

This study primarily focuses on the physical and chemical adsorption of hazardous contaminants using MOFs. The review is conceptually divided into four main sections:

(1) ***Overview of environmental pollutants and adsorbent materials***: In the first section, we provide an overview of different types of environmental pollutants and summarize the organic and inorganic materials commonly employed as adsorbents for pollutant adsorption and extraction.
(2) ***Adsorption of harmful gases, VOCs, and toxic metals***: The second section delves into the adsorption of harmful gases, VOCs, hazardous organic compounds, and toxic metals, considering size limitations and the interactions between the adsorbates and MOF surfaces.
(3) ***Strategies for enhancing adsorption capacity***: The third section explores strategies to optimize the adsorption capacity, considering various factors such as functionality, moisture, coordinated unsaturated metal cations, acidity, basicity, and MOF defects, all of which significantly influence the adsorption process.
(4) ***Addressing challenges and future research directions***: Lastly, we address and illustrate the challenges faced in this field and present our perspective on the future research directions for MOFs.

In this review, the focus is on highlighting the global relevance and significance of research on MOFs in the context of addressing pressing global challenges. MOFs have emerged as highly promising materials for a wide range of applications, including adsorption, catalysis, and environmental remediation. These versatile materials offer unique advantages, such as high adsorption potential, large surface area, tunable porosity, and recyclability, making them invaluable tools for mitigating environmental contamination.

By carefully selecting metal ions and organic linkers, the efficiency and selectivity of MOFs for the removal of specific contaminants can be controlled, aligning with key United Nations Sustainable Development Goals (UNSDGs). Specifically, this work contributes to UNSDG 6 (Clean Water and Sanitation), UNSDG 13 (Climate Action), UNSDG 14 (Life Below Water), and UNSDG 11 (Sustainable Cities and Communities). By addressing water pollution, reducing greenhouse gas emissions, improving air quality, and advancing sustainable urban development, this research highlights the potential for MOFs to play a pivotal role in achieving these global goals.

The growing body of research in this area underscores the emerging value of MOFs in environmental applications and provides insights for the development of efficient treatment technologies to combat hazardous environmental emissions on a global scale.

2. Environmental pollutants and organic/inorganic materials for removal of pollutants

2.1. Environmental pollutants

The hazardous wastes that pose a significant threat to the global aquatic system can be categorized into four main groups: (i) Aquatic pollution, (ii) hazardous inorganic wastes, (iii) hazardous organic wastes, and (iv) commercial chemical products.

2.1.1. Aquatic pollution

Clean water is an essential and vital resource that fulfils the needs of various sectors in human society, including drinking, washing, farm irrigation, and industrial development. Unfortunately, the wasteful consumption of clean water and the negligent management of wastewater from households and businesses have resulted in severe contamination of natural aquatic environments. Water contamination can be broadly classified into two categories: point sources and non-point sources [40]. Point sources involve the release of toxins into water bodies from factories, septic materials, animal feedlots, mines, oil plants, and other similar sources. Non-point sources include agricultural runoff, sedimentation, animal waste, and various other factors [41]. The presence of these contaminants in water supplies can lead to significant environmental problems and pose risks to public hygiene and health [42]. For example, the pollution of groundwater by pesticides can pose a threat to aquatic ecosystems. Discharging fertilizers into water bodies can cause an overgrowth of algae, disrupting oxygen levels and disturbing the ecological balance of the water system. Moreover, direct contact with or consumption of polluted water can result in skin rashes and serious diseases in humans, such as typhoid fever and gastrointestinal ailments. Inorganic and/or organic chemical waste, particularly heavy metal ions, can be adsorbed by fish in the water, leading to contamination.

2.1.2. Inorganic wastes

2.1.2.1. Anionic waste

The most predominant contaminants in polluted surface water are phosphates and nitrates. The application of large quantities of P and N-containing fertilizers to the soil leads to a substantial accumulation of soil phosphates and nitrates. The application to the field of large quantities of fertilizers containing P and N results in a substantial accumulation of phosphates and nitrates in the soil. Phosphates and nitrates can penetrate groundwater and surface reservoirs, such as rivers and lakes, due to natural precipitation. Water contamination of nitrates jeopardizes the health of people and other animals. High nitrate concentrations in water are highly toxic. While phosphorus is not as harmful in water as nitrate, it can promote the growth of algae in water along with nitrate contaminants. Their extreme discharge into sources of surface water will lead to serious eutrophication of the sources of surface water. The most commonly observed effect of eutrophication is that it induces the reproduction of marine algae and vegetation, allowing water in aquatic environments to smell and taste, and avoiding the use of toxic environments as a source of drinking water for industry, agriculture and humans. Another important class of anionic pollutants is cyanides. Cyanide salts such as sodium cyanide and potassium cyanide or as hydrogen cyanide in the gas process can be derived from natural sources are usually available. Cyanides from neglected industrial wastewater, coal gasification, electroplating, and partial burning of fuels can be emitted into the water supply [43,44].

2.1.2.2. Cationic waste

Heavy metal ions such as iron, arsenic, mercury, chromium, nickel, barium, cadmium, cobalt, selenium and vanadium are the most common inorganic cationic wastes identified in marine environments and soil. Human/industrial operations, such as manufacturing of printed circuits and semiconductors, finishing and coating of metals, industrial painting techniques, etc., are the major sources of heavy metal contaminants. These heavy metal ions, if highly exposed and indirect contact, are lethal and can poison people and animals. Acute and chronic signs can be subdivided as evidence of heavy metal poisoning in humans. Anxiety, dyslexia, decreased focus, migraines are chronic signs. It is necessary to eliminate ionic heavy metal contaminants from the water supply for the reasons specified [44–46].

2.1.3. Organic wastes

Chemical contaminants derived from harmful organic molecules can cause extreme illness in humans at large concentrations. These organic compounds come from a wide range of consumer materials that can be used in a wide variety of settings, such as detergents, refined hydrocarbons, chemicals, organic solvents, pesticides, and dyes. Moreover, due to their long-term adverse consequences and chemical complexity, these biological contaminants pose a threat to ecosystems and humans. Specifically, thousands of persistent organic contaminants are a class of chemicals consisting of a heterogeneous group of bioaccumulating toxic organic compounds and are subject to long transport routes [47,48]. They are emitted from urban and industrial waste, landfills, farming activities, and other sources into the atmosphere and undergo multiple reactions that validate their prevalence.

The primary surface drainage of aliphatic organic compounds is highly prevalent in urban environments. Aliphatic compounds are primarily by-products of petroleum combustion and serve as toxic contaminants in the aquatic environment, mainly through surface runoff. Various aliphatic organic compounds, including alkenes, alkynes, dichlorodifluoromethane, dichloromethane, propanol, and tetramethylammonium ions, have been reported.

Another type of organic material that is released into the atmosphere by the incomplete combustion of organic substances, such as wood, charcoal, and oil, is polycyclic aromatic hydrocarbons. The extensive use of polychlorinated biphenyls in many manufacturing processes increases their entry into the atmosphere through electrical transformers, capacitors, carbonless paper, and plastics.

Another category of organic compounds used in various chemical frameworks is pesticides, which are used for diverse agricultural and non-agricultural purposes, including herbicides, insecticides, fungicides, and germicides. Dyes are colored compounds that are closely related to the substrates to which they are added. Numerous manufacturing methods, such as the production of herbicides, plastics, textile precursors, photo producers, dyes, pharmaceuticals, and the pulp and paper industry, result in the by-products of phenol and phenolic compounds.

Moreover, the incomplete mineralization of phenolic compounds contributes to natural organic by-products, which are commonly dispersed in our environment, including humic substances, lignins, and tannins. The toxicity of phenols and phenolic derivatives is primarily due to the rapid release of free electrons that create intermediates and phenoxy radicals [49–51].

2.2. Organic-based materials as innovative adsorbents for removal of pollutants from the environment

Activated carbons, carbon nanotubes, graphene, zeolite, and organic polymers, which are often formed by pyrolysis of materials with rich carbon content, are possibly the most common porous materials intensively exploited. They have high surface areas and a high potential for adsorption implicitly.

2.2.1. Isotherm model

Adsorption isotherms play a crucial role in studying the adsorption capacities of adsorbents. They provide valuable insights into the relationship between the equilibrium concentrations of the adsorbates and the amount of adsorbates on the adsorbents at a constant temperature. An adsorption isotherm is determined by measuring the adsorption equilibrium under constant temperature conditions [52].

2.2.1.1. Langmuir model

Adsorption occurs consistently at the active sites of the adsorbents, according to the Langmuir model. Adsorption activity ceases at these sites as soon as they are filled by the adsorbates. The Langmuir model postulates that every active adsorption site possesses identical binding energy, and each site can accommodate only a single adsorbate. The Langmuir model's linear form is expressed in Eq. (1) [53]:

$$\frac{C_e}{q_e} = \frac{1}{bq_m} + \frac{C_e}{q_m} \tag{1}$$

where C_e represents the equilibrium concentration of the adsorbate (mg·L^{-1}), q_e is the equilibrium adsorption capacity (mg·g^{-1}), q_m is the maximum adsorption capacity of a single layer (mg·g^{-1}), and b denotes the equilibrium constant.

2.2.1.2. Freundlich model

The Freundlich isotherm offers a scientific equation that effectively elucidates non-ideal adsorption phenomena. This model corresponds to the exponential distribution of heterogeneous surfaces often encountered in active centers. The Freundlich model is based on multilayer adsorption, as opposed to the Langmuir model, and its linear structure can be expressed by Freundlich [54]:

$$\ln q_e = \left(\frac{1}{n}\right)\ln C_e + \ln K_F \tag{2}$$

where C_e is the equilibrium concentration of the adsorbate (mg·L^{-1}), q_e is the equilibrium adsorption capacity of the adsorbent (mg·g^{-1}), K_F is the Freundlich constant (index of adsorption capacity), and n is also a Freundlich constant (index of adsorption intensity or surface heterogeneity).

2.2.1.3. Sips isotherm model

The Sips isotherm model is often used to describe multilayer adsorption onto heterogeneous surfaces. The non-linear equation is given by Ho et al. [53]:

$$q_e = \frac{q_m K\left(C_e\right)^n}{1 + K\left(C_e\right)^n} \tag{3}$$

where C_e is the equilibrium concentration of the adsorbate (mg·L^{-1}), q_e is the equilibrium adsorption capacity of the adsorbent (mg·g^{-1}), q_m is the maximum adsorption capacity (mg·g^{-1}), K is the Sips equilibrium constant, and n is the heterogeneity parameter.

2.2.1.4. Temkin isotherm model

The Temkin isotherm model is used to describe adsorption on a heterogeneous surface, considering interactions between adsorbate molecules. The non-linear equation is given by Ho et al. [53]:

$$q_e = \frac{RT}{b_T}\ln A_T C_e \tag{4}$$

where C_e is the equilibrium concentration of the adsorbate (mg·L^{-1}), q_e is the equilibrium adsorption capacity of the adsorbent (mg·g^{-1}), R is the gas constant, T is the absolute temperature, b_T is a constant related to adsorption enthalpy, and A_T is the Temkin constant related to the heat of adsorption.

2.2.1.5. Dubinin–Radushkevich isotherm model

The Dubinin–Radushkevich isotherm model is commonly used for the characterization of microporous adsorbents. The non-linear equation is given by Ho et al. [53]:

$$q_e = q_m \exp\left(-\beta\varepsilon^2\right) \tag{5}$$

where q_e is the equilibrium adsorption capacity of the adsorbent (mg·g^{-1}), q_m is the maximum adsorption capacity (mg·g^{-1}), ε is the Polanyi potential, β is the Dubinin–Radushkevich constant, related to the energy of adsorption.

2.2.2. Activated carbon-based adsorbents

A wide range of raw materials with a high carbon/ash content, such as tar, lignite, or coconut, can be used to produce activated carbon (AC). The manufacturing process is highly energy-consuming and typically proceeds: a gradual increase in temperature to 500°C oxidizes and eliminates volatile impurities. Further heating to 1,000°C generates steam, which expands the material's porous structure. During the activation process, a variety of pore sizes is created, ranging from the carbon surface to the particles. Pore sizes are categorized into three groups based on the diameter of the pore openings [55].

It is well known that granular activated carbon has the potential to extract a large range of organic compounds from water. Factors associated with the tremendous increase in the development of organic chemicals have affected the efficiency of many water supplies in recent decades. Many toxins are strongly stabilized organic compounds that are not eliminated by the disposal of biological or chemical waste and also survive the self-cleaning that typically takes place in wetlands. In water treatment schemes, organic compounds are not greatly separated from the coagulation, chlorination and filtration procedures used. To make the water tasty and avoid foaming, activated carbon is used in adequate amounts and only the most fragrant additives give a palpable taste to the dilutions usually present. It is more adsorbable to certain organic toxins than others. Due to their poor water solubility, organic solvents such as trichloroethylene and aromatic solvents such as toluene are adsorbable. It also successfully adsorbs high molecular weight compounds such as polynuclear aromatics and surfactants. Water-soluble molecules including alcohols and aldehydes are poorly adsorbed, on the other hand. Generally, VOCs such as chlorinated solvents and aromatics with low molecular weight are treated with granular activated carbon. However, the incorporation of VOCs into the atmosphere restricts their use for environmental purposes. Granular activated carbon, on the other hand, can eliminate volatile and non-volatile chemicals, minimize chemical emissions rapidly to undetectable limits and avoid their return to the environment [56–60].

Activated carbon, owing to its well-developed pore structure and high inner surface for adsorption, is a strong adsorbent for adsorbing toxic metals. However, because activated carbon based on coal is costly, its use has been reduced and more attempts have been made to turn inexpensive and plentiful agricultural waste into activated carbon. Anirudhan and Sreekumari [61] have shown that chromium is extracted from wastewater and have demonstrated positive results. Owing to their harmful effects, the removal of such dangerous metals such as lead (Pb) and cadmium (Cd) is very urgent. As stated by Ullah et al. [62], the removal efficiency of both metals was highly dependent on their initial concentration, contact time, pH, temperature and adsorbent quantity.

2.2.3. Carbon nanotubes as adsorbent

They have undoubtedly revolutionized the field of nanotechnology since the invention of carbon nanotubes (CNT). CNTs are cylindrical macromolecules with a radius of a few nanometers and a length of up to many micrometers, as defined by Iijima [63] and Bethune et al. [64]. The walls of these tubes consist of a hexagonal network of carbon atoms and are covered by fullerene-like structures. The unique structure of CNTs can primarily be categorized into multi-walled carbon nanotubes and single-walled carbon nanotubes. Across various technical domains, several solutions have been proposed to harness the exceptional physical, chemical, and electronic properties of CNTs. Impurities found in wastewater, such as heavy metal ions, 1,2-dichlorobenzene, and dioxin, are non-degradable, highly toxic, and carcinogenic. They can lead to cumulative toxicity, cancer, and nerve damage [63–66]. The elimination of these impurities relies on the adsorption behavior of an adsorbent. Carbon nanotubes (CNTs) exhibit outstanding adsorption capabilities and superior adsorption performance compared to traditional granular and powdered activated carbon, which have limited properties, such as surfactant sites and activation energy, due to their high surfactant site/volume ratio and controlled pore size distribution. Extensive experiments have demonstrated that both the surface functional groups and the nature of the sorbate are factors affecting the adsorption potential of CNTs. For example, the presence of surface acidity (carboxyl, lactone, and phenolic groups) facilitates the adsorption of polar compounds [67]. On the other hand, it has been observed that the surface of non-functionalized CNTs has a higher potential for adsorbing non-polar compounds, such as polycyclic aromatic hydrocarbons, compared to polar compounds. Chemical interactions with polar compounds and physical interactions with non-polar compounds primarily involve the diffusion activity of CNTs. Langmuir or Freundlich isotherms are typically used to describe the adsorption of polar and non-polar compounds [68,69].

Across a broad pH range, CNTs exhibit effective adsorption capabilities. Adsorption and desorption experiments have shown the reliability of CNTs for various adsorption and desorption cycles. In a regeneration study, Lu et al. [70] reported that metal adsorption and desorption in CNTs decreased marginally, whereas in granular activated carbon (GAC), it decreased significantly after a series of cycles. This phenomenon can be attributed to the porous structure of GAC, which makes it difficult to desorb metals, requiring ions to travel from the inner surface to the outer surface of the pores [70].

In addition to their role as adsorbers for organic and inorganic pollutants, recent research has explored the use

of CNTs as nanofilters to reduce particle concentration in wastewater. Similar to adsorbents, the specific selectivity of CNT filters can be customized by incorporating various functions at the pore inlets. CNTs have demonstrated excellent efficiency in water transport, owing to their hydrophobic properties [71]. Molecular dynamics simulations reveal that the hydrophobic nature of CNT pores results in weak interactions with water molecules, allowing for rapid and nearly normal water flow.

The application of CNTs in wastewater treatment extends beyond filtration and adsorption. Several studies have shown that CNTs possess strong antimicrobial properties, enabling them to serve as an effective alternative to chemical disinfectants in combating microbial infections. The use of CNTs in water disinfection helps prevent the formation of hazardous disinfection by-products, such as trihalomethanes, haloacetic acids, and aldehydes, as CNTs are not potent oxidizing agents and remain relatively inert in water [72].

2.2.4. Graphene as an adsorbent

Graphene, the first 2D crystal, is an essential nanomaterial used for extracting heavy metals from wastewater due to its outstanding properties, such as stiffness, elasticity, mechanical strength, thermal and electrical conductivity, as a carbon-based material [73]. Furthermore, two categories of nanomaterials derived from graphite that can also be applied to extract heavy metals from effluent are graphene oxide (GO) and reduced graphene oxide (rGO) [74]. GO serves as a graphene oxidation agent and contains numerous functional groups rich in oxygen, including epoxy, carboxyl, carbonyl, and hydroxyl, which aid in the removal of heavy metals. In general, the reduction product of graphene oxide (rGO) tends to exhibit a higher number of defects compared to pristine graphene. Additionally, rGO is more susceptible to modifications by functional groups such as COOH, OH, and others [75]. The removal of heavy metals from graphene-based nanomaterials is attributed to their unique combination of properties, including size, specific surface characteristics, and various functional groups such as COOH, OH, and CH(O)CH, among others. These remarkable features play a significant role in the removal mechanism [76].

The density of fillers and their extremely hydrophilic properties make graphene and GO/rGO materials common choices for extracting heavy metals from wastewater. For example, Qin et al. [77] conducted batch experiments to analyze the performance factors of GO adsorption in heavy metal removal, including pH, adsorbent dosage, temperature, and contact time, and found that the adsorption mechanism aligned well with the kinetic pattern of the Langmuir isotherm and the pseudo-second-order kinetics, demonstrating GO's high Zn(II) adsorption capacity. Zhao et al. [78] synthesized multilayer graphene oxide nanosheets using a modified Hummers process and employed a batch process to adsorb Co(II) and Cd(II) from water. They observed that the adsorption process was significantly influenced by pH, and the presence of humic acid in a water-based solution reduced the adsorption of Cd(II) and Co(II). The study also examined the thermodynamic parameters of this adsorption process, revealing that the adsorption of Co(II) and Cd(II) on GO nanosheets is both endothermic and spontaneous.

Furthermore, graphene-based nanocomposites are increasingly being used to extract heavy metals from aqueous solutions. The well-dispersed nature of GO in water makes it difficult to isolate from the solution [78]. Recently, Arshad et al. [79] synthesized a new graphene-modified adsorbent to improve the adsorption potential for heavy metals. They integrated calcium alginate spheres into graphene oxide and further reduced them with polyethyleneimine. Batch adsorption experiments were conducted in a shaking bath. According to the Langmuir isotherm, the adsorption capacities of this GO-based nanocomposite were ranked as Pb(II), Hg(II), and Cd(II), indicating its superior performance in extracting these three ions. The adsorption kinetics followed pseudo-second-order kinetics, and the parameters of thermodynamic adsorption indicated that the mechanism of adsorption could be attributed to physico-chemical adsorption. Reusability tests of the adsorbent demonstrated excellent Pb(II) removal efficiency even after five cycles.

Vilela et al. [80] are developing new microbots (GOx microbots) based on graphene oxide that could serve as self-propelled devices for capturing, transporting, and removing heavy metals. Most work on graphene-based nanomaterials, however, remains at a preliminary research stage, with a lack of research into the practical application of graphene-based nanomaterials for industrial wastewater treatment, especially in the case of wastewater containing multiple pollutants. Furthermore, the economic feasibility of recycling and reusing graphene-based nanomaterials requires further study.

2.2.5. Zeolite as an adsorbent

Zeolites are aluminosilicate microporous minerals widely utilized as industrial catalysts and adsorbents [81]. Their versatile properties find applications in various sectors, including industry, agriculture, medicine, chemical technology, environmental protection, and engineering [82]. Zeolites are employed in diverse processes, such as reactions with organic compounds (separation of unsaturated hydrocarbons and selective adsorption of petroleum substances and other organic molecules with molecular sieving properties). They are often used in treating acidic wastewater generated during the production of monochloroacetic acid from chlorinated organic compounds or in the removal of phenols from wastewater. Additionally, zeolites are employed in various applications, including membranes, molecular sieves, and the elimination of gaseous contaminants in wastewater treatment, as well as in the nuclear industry [83,84]. They serve as efficient ion exchangers, and their applications extend to medication and gas separation.

Zeolites are commonly harnessed in water treatment, wastewater technologies, and the purification of flue gases for environmental purposes. They possess the capability to remove substantial quantities of pollution-inducing ions, including radionuclides such as ^{137}Cs and ^{90}Sr, metals, ammonium ions, chloroform, and carbon tetrachloride from acidic wastewater [85]. In the context of heavy metal adsorption, zeolites exhibit distinct selectivity for this category of contaminants commonly found in water, waste, or sludge [86]. Querol et al. [82] conducted a study on the removal of heavy metals from iron- and aluminum-rich polluted water,

where synthetic zeolites demonstrated excellent selectivity: Al^{3+}, Fe^{3+}, Pb^{2+}, Cu^{2+}, Cd^{2+}, Zn^{2+}, Ti^{+}, Mn^{2+}, Mg^{2+}, Ca^{2+}, Sr^{2+}. Lee et al. [87] examined the selective adsorption of Zn, Cu, Cd, and Pb cations for both natural and synthetic zeolites, revealing that synthetic zeolites exhibited greater cation exchange capacity and thus higher heavy metal cation adsorption [87].

Zeolites are frequently employed to decontaminate floors, gases, and aqueous solutions from mercury emissions, in addition to other cost-effective adsorbents [88,89]. To capture mercury in vapor phases, a high-temperature resistant synthetic zeolite impregnated with silver has been developed [90]. Moreover, this zeolite has demonstrated a high selectivity against dioxins, furans, and other polycyclic hydrocarbons, which undergo thermal decomposition following the initial mercury vapor capture. Zeolites are most effective in extracting compounds such as SO_2, CO_2, CO, NO_x, H_2S, and NH_3 [90,91].

2.2.6. Nanocomposites supported by organic polymers

Polymer hosts possess numerous distinctive properties that make organic polymers a competitive choice for nanocomposite hosts. These properties include tunable functionality, excellent mechanical strength, regenerative capacity, environmental resilience, and degradable characteristics [92]. There are two main categories of polymer-based nanocomposites: synthetic organic polymer-based nanocomposites and biopolymer-based nanocomposites [93]. Polymer nanocomposites can be produced using two methods: direct assembly and in situ synthesis [94]. Synthetic organic polymers such as polyaniline and polystyrene are commonly used in the production of nanocomposites for the removal of heavy metals [95]. For instance, Afshar et al. [96] developed a magnetic nanocomposite of polypyrrole-polyaniline/Fe_3O_4 and studied its ability to extract Pb(II) from aqueous solutions. At pH levels between 8 and 10, these nanocomposites were able to extract nearly 100% of the Pb(II). The isothermal model and the second-order pseudo-model of Freundlich provided a better fit for the adsorption data.

Biopolymers, such as cellulose, chitosan, and alginate, are widely used as matrices for nanocomposites, in addition to synthetic organic polymers. Cellulose, one of the most common biopolymers, has hydroxyl groups on its glucose rings, providing multiple binding sites for heavy metal ions [97]. Therefore, it is a promising raw material for adsorbents. Suman et al. [98] developed a silica-based composite material embedded in nanocellulose (NC)-Ag (AgNP) nanoparticles using advanced techniques for the extraction of dyes, heavy metals, and microbes from water. The results indicated successful removal of almost all Pb(II) and Cr(III) and efficient microbial load decontamination.

Saad et al. [99] synthesized a ZnO/core-shell chitosan nanocomposite, which is cost-effective and has lower biological toxicity. This nanocomposite was tested for its ability to extract Pb(II), Cd(II), and Cu(II). The batch adsorption results showed high adsorption capacities for Pb(II), Cd(II), and Cu(II) according to the Langmuir isothermal model, making it an excellent adsorbent with the capability for repeated use.

Gokila et al. [100] reported the development of a chitosan/alginate nanocomposite for the removal of Cr(VI) from wastewater. The batch adsorption experiments demonstrated promising adsorption capabilities for Cr(VI), with the adsorbent showing a preference for multilayer adsorption.

Lofrano et al. [101] provided a detailed description of functional polymer nanocomposites (PFNCs) for the removal of metals from water. Their work covered planning, analysis, toxicity, interactions between PFNCs and removal of nanoparticles, and polymer hosts.

While polymer nanocomposites have demonstrated their effectiveness for the removal of heavy metals, further research is warranted to enhance the synthesis process, reduce costs, develop recovery techniques, and ensure environmental protection, among other factors [101].

3. MOFs-based materials for the removal of pollutants from the environment

MOFs stand out as one of the most potent porous materials for addressing environmental contamination. They are recognized for their ability to form network-structured porous materials by self-organizing complex structures from organic ligands and metal ions. MOFs employ various adsorption processes, such as open metal sites, electrostatic adsorption, π–π bonds, hydrogen bonding, and acid–base interactions, to achieve highly effective contaminant removal [102]. These materials are believed to offer advantages over conventional porous materials, holding great promise for diverse applications in this field [103].

However, it is important to note that the production of MOF materials is not a straightforward process. The composition of MOFs during their synthesis is greatly influenced by various factors, including the coordination compound, the coordination environment, central metal ions, and organic ligands [104]. Among these factors, parameters like temperature, the molar ratio of metal ions to organic ligands, the choice of solvent, the pH of the reaction, the concentration of components, and the reaction duration play a significant role in determining the structure and efficiency of the resulting MOFs. Therefore, addressing these critical reaction conditions is essential in the quest for optimizing MOFs for environmental applications [105,106].

Various synthetic methods can be employed in the fabrication of MOFs. The conventional solution process involves the combination of metal components, organic ligands, and other raw materials in a specific solvent. This mixture is then subjected to specific temperature and duration conditions, as illustrated in Fig. 1, outlining the MOF synthesis process. Subsequently, the reaction product is obtained through filtration, followed by solvent evaporation to yield purified MOF crystals [107,108].

The hydrothermal or solvothermal process (Fig. 2) involves combining metal ions, organic binders, reaction solvents, regulators, and other precursors in specific proportions. This mixture is then placed in a high-temperature reactor to initiate a reaction at a predetermined temperature. As soon as the reaction is complete, the reactor's temperature is gradually reduced to ambient or room temperature using water. The resulting sample is subjected to multiple cleaning steps to eliminate impurities. Subsequently, the product is washed once more using anhydrous ethanol or alternative

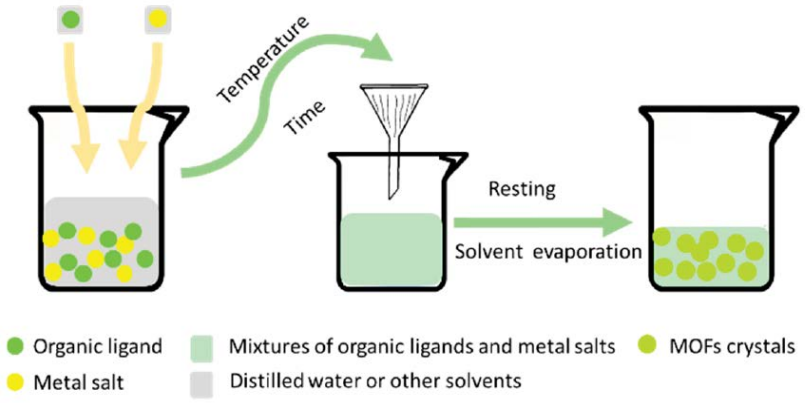

Fig. 1. Schematic diagram illustrates the conventional solution methods used for synthesizing metal–organic frameworks. Reproduced with permission from MDPI ref. [106] (Creative Commons CC BY license).

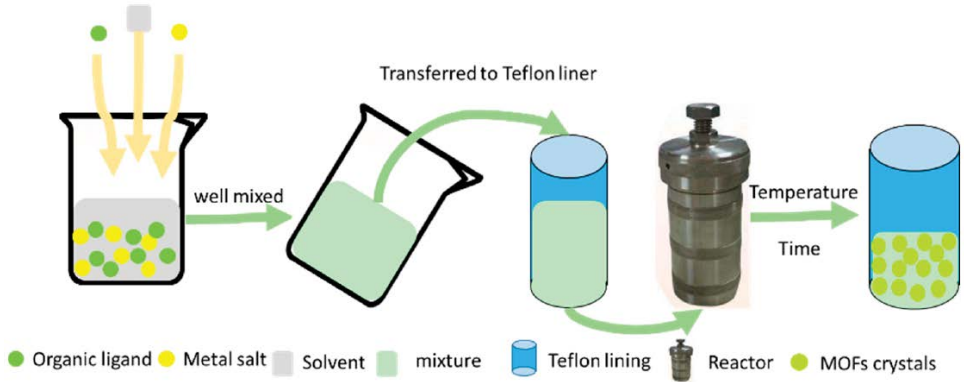

Fig. 2. Schematic diagram illustrates the synthesis of metal–organic frameworks using the hydrothermal/solvothermal method or solvent heating methods. Reproduced with permission from MDPI ref. [106] (Creative Commons CC BY license).

solvents at a fixed temperature. Pure MOF can be obtained after vacuum drying [109].

Porous coordination polymers can be categorized into three generations (Fig. 3): the 1st, 2nd, 3rd, and 4th generations [110]. The 1st generation PCPs have microporous frameworks that are maintained solely by guest molecules and experience irreversible structural collapse after the removal of these guest molecules. The 2nd generation PCPs feature stable and robust frameworks akin to zeolites, retaining permanent porosity even after the evacuation of guest molecules from their cavities. The 3rd generation PCPs possess flexible frameworks with a certain degree of dynamicity in response to various external stimuli, such as guest molecules, electric fields, pressure, and light. They can undergo reversible modifications of their cavities. Many inorganic porous compounds, constructed through covalent bonds, fall into the category of 2nd generation materials. The concept of the 4th generation MOFs is closely linked to the advancement of post-synthetic modifications (PSM) of MOFs. These modifications involve post-processing MOFs in a way that preserves their topology and structural integrity, allowing for various subsequent modifications to be made [111,112].

Hybrids, such as PCPs or MOFs, leverage their ordered structure, increased stability, and significantly higher specific surface areas. Fig. 4 provides a brief overview of potential applications in gas storage, gas/vapor separation, catalysis, luminescence, magnetism, and drug storage and delivery [114].

3.1. MOFs for the removal of harmful gases

Efficiently capturing hazardous chemicals is of significant value, both for environmental preservation and for the protection of individuals at risk of chemical exposure. However, the utilization of MOFs alone for capturing harmful gases and addressing more complex interactions between noxious adsorbates is often limited due to the restricted pore size and shape of MOFs. To enhance the selectivity and adsorption efficiency of MOFs for specific toxic compounds, certain strategies can be employed (Fig. 5), such as introducing open metal sites (coordinated unsaturated metal centers) on the surface of the pores or functionalizing MOFs. This can be achieved through coordination bonds, acid-based interactions, and the formation of π complexes or hydrogen bonds. It is important to note that in addition to the mentioned processes, hydrogen bonding and breathing effects also play a crucial role in the adsorption of toxic gases in MOFs.

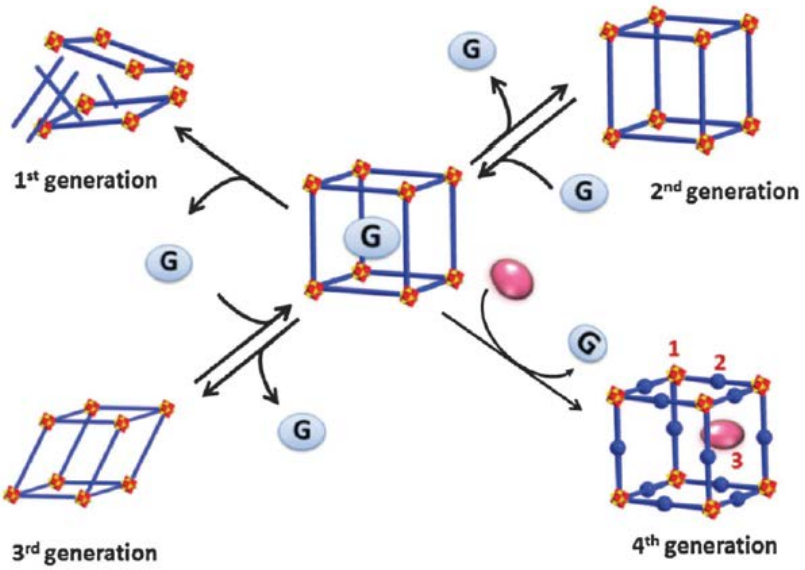

Fig. 3. Classification of MOFs into different generations. In the 1st generation, MOFs collapse when guests are removed. The 2nd generation MOFs possess permanent porosity that remains unaffected by guest removal. The 3rd generation MOFs exhibit flexible and dynamic properties. Finally, the 4th generation MOFs are capable of sustaining post-processing modifications, allowing for modifiable positions at metal/cluster sites, organic linkers, and vacant spaces. Reproduced with permission from RSC ref. [113] (License ID 1406562).

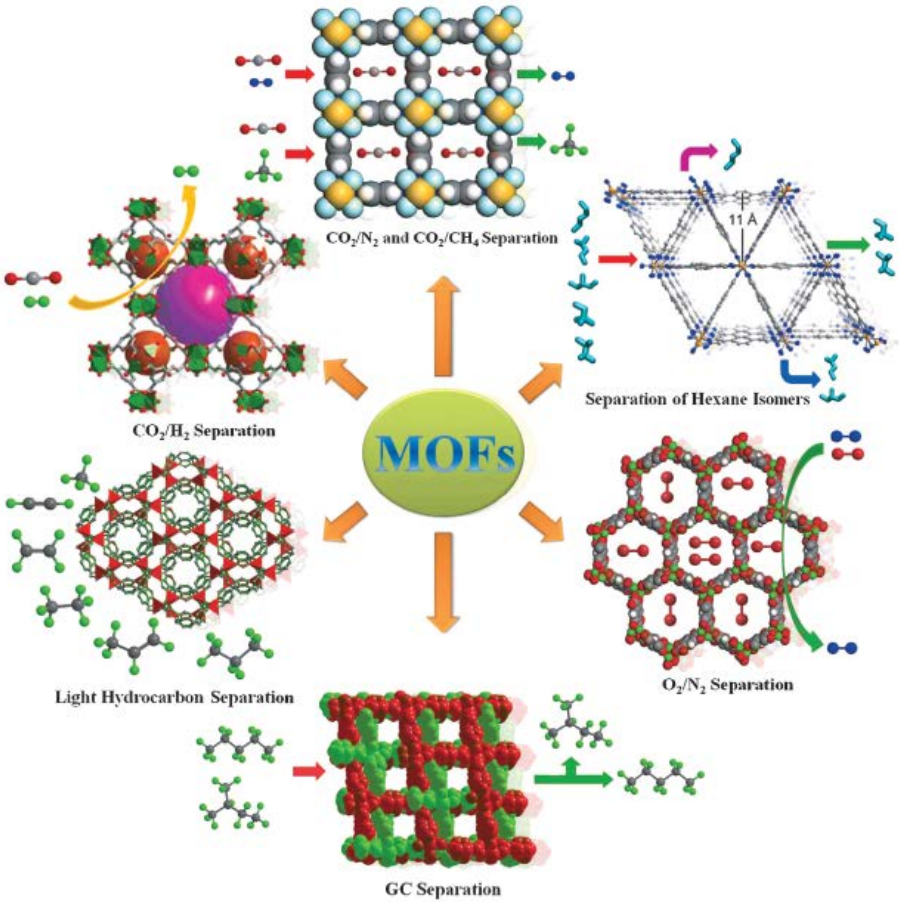

Fig. 4. MOFs exhibit a diverse array of environmental applications. Reproduced with permission from Elsevier ref. [115] (License ID 5647840063660).

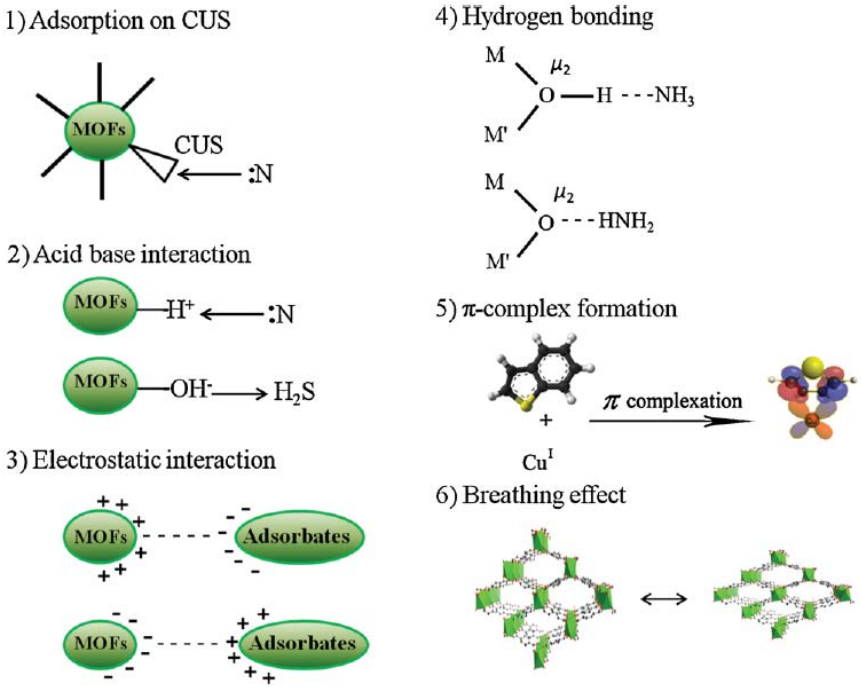

Fig. 5. Significant mechanisms involved in the adsorption of toxic gases (NH_3, H_2S). Reproduced with permission from Elsevier ref. [21] (License ID 5647830101875).

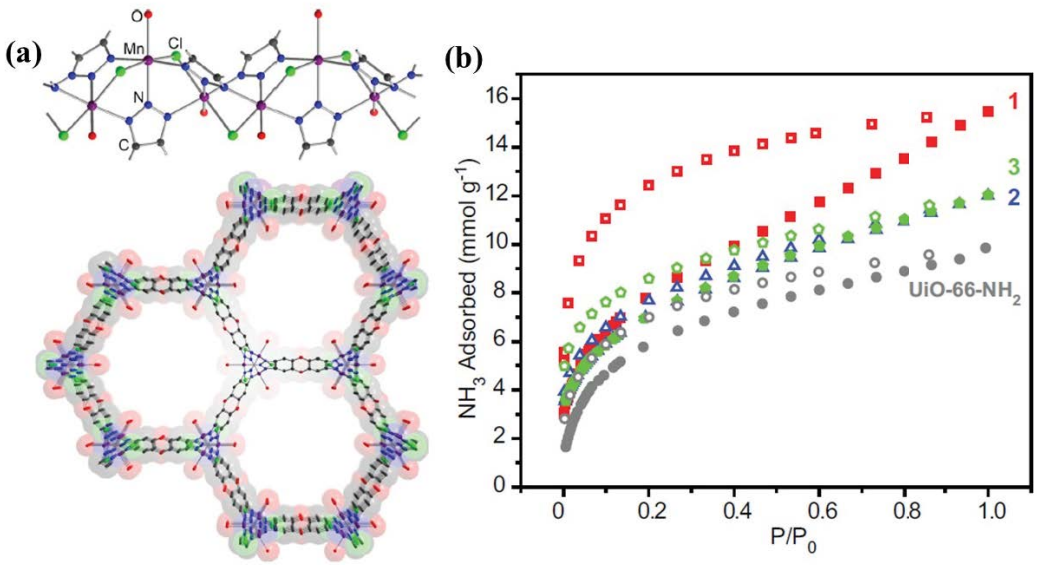

Fig. 6. (a) Secondary building unit (top) and structure viewed along the *c*-axis (bottom) of $M_2Cl_2(BTDD)(H_2O)_2$ and (b) NH_3 adsorption isotherms of $Mn_2Cl_2(BTDD)(H_2O)_2$ (1, red squares), $Co_2Cl_2(BTDD)(H_2O)_2$ (2, blue triangles), $Ni_2Cl_2(BTDD)(H_2O)_2$ (3, green pentagons), and UiO-66-NH_2 (grey circles) at 1 bar, 298 K. Reproduced with permission from ACS ref. [121] (License ID 1647347).

3.1.1. NH_3 removal

Several industries, including pharmaceuticals and fertilizer production, are involved in the manufacturing of various goods, such as cleaning products. Annually, they generate an estimated 150 million tons of NH_3, a crucial raw material. NH_3, a toxic chemical, has been recognized and listed in NATO's Threat Index due to its harmful characteristics and associated risks in processing and storage [116,117]. Developing new materials for the adsorption of NH_3 from the air is of considerable importance, considering the potential for acute and chronic NH_3 exposure. MOFs are considered a promising adsorbent for NH_3. A previous study demonstrated that HKUST-1 (HKUST stands for Hong Kong University of Science and Technology) efficiently adsorbs NH_3 in both dry and wet environments [118]. The mechanism

relies on NH_3 molecules acting as Lewis acid/base and coordinating with open Cu(II) sites. In their research, Kobielska et al. [119] chose Cu_2(dobdc) due to its high Cu(II) site density (4.7 nm^{-3}) among all MOFs, exhibiting exceptional selectivity for NH_3 while effectively adsorbing it. Cu_2(dobdc) demonstrates NH_3 sorption levels of 7.6 and 3.4 $mmol \cdot g^{-1}$ under 80% and 0% relative humidity, respectively. Although the adsorption per Cu site and gravimetric NH_3 molecules are lower compared to HKUST-1, Cu_2(dobdc) outperforms HKUST-1 in volumetric sorption at 5.9 NH_3/nm^3, particularly at 80% relative humidity [120]. Rieth et al. [121] provided details on the synthesis of various MOFs (Fig. 6), $M_2Cl_2(BTDD)(H_2O)_2$ (M = Mn, Ni, and Co; BTDD = bis(1H)-1,2,3-triazole[4,5-b],[4′,5′-i])dibenzo-1,4-dioxin, which rely on highly stable azolates and exhibit NH_3 adsorption properties. NH_3 removal from $Mn_2Cl_2(BTDD)(H_2O)_2$, $Co_2Cl_2(BTDD)(H_2O)_2$, and $Ni_2Cl_2(BTDD)(H_2O)_2$ at 1 bar and 298 K was recorded at 15.47, 12.00, and 12.02 $mmol \cdot g^{-1}$, respectively. It's worth noting that high NH_3 adsorption is reversible over at least three cycles. UiO-66-NH_2 showed an initial adsorption of 9.84 $mmol \cdot g^{-1}$ but exhibited substantial crystallinity loss, losing more than 50% of its original ammonia capacity after three successive adsorption cycles [121].

A computer screening of MOFs groups, as evaluated by Kim et al. [122], has shown that binding NH_3 to coordinate metals with linker functionalities can be useful. It was determined that RCOOCu groups achieve the most favorable binding energies with ammonia among all functionalities [122]. Joshi et al. [123] successfully integrated copper into various UiO-66 analogues with carboxylic acid functional groups, including UiO-66-$(COOCu)_2$, UiO-66-COOCu, and UiO-66-oxCu, using a post-synthesis modification technique. Innovative studies involving NH_3 under both dry and wet conditions (80% relative humidity) revealed that the two materials investigated exhibited a significant enhancement in the dynamic adsorption capacity of NH_3. The novel material UiO-66-$(COOCu)_2$ demonstrated a dynamic NH_3 capacity exceeding 6 $mmol \cdot g^{-1}$ in both humid and dry environments while maintaining its stability under both wet and dry conditions.

For gas separation and air filtration applications, it is essential to incorporate MOF crystallites into solid and easily handled support materials, enabling their efficient use as adsorbents. According to Padial et al. [124], they investigated the application of chitin-based matrices derived from a marine sponge as a supporting material for MOF deposition. Through powder X-ray diffraction measurements, they confirmed the even distribution of HKUST-1 within the matrix, with no formation of crystalline by-products. The ammonia isotherm adsorption data showed that NH_3 has an adsorption capacity of 39 $mg \cdot g^{-1}$, which is approximately 40% of the capacity observed for pure HKUST-1 (97 $mg \cdot g^{-1}$).

3.1.2. Benzene removal

In a large number of chemical and industrial processes, benzene and its derivatives can be utilized for different purposes and may be discharged into the environment. The release of these organic pollutants, however, would raise several health concerns. For the mitigation of benzene, the use of porous materials with reversible physisorption offers a promising solution. MOFs have been studied as a new class of porous materials suitable for the adsorption of benzene and its derivatives. The amount of benzene adsorbed on HKUST-1, for instance, reached 10.0 $mmol \cdot g^{-1}$ at 1.0 kPa and 298 K [125]. Adsorption of benzene was 2.6 $mmol \cdot g^{-1}$ at 0.69 kPa and 303 K at MIL-141 (Cs) (MIL stands for Materials Institute Lavoisier) [126]. The adsorption of toluene to SCUTC-18 (SCUT stands for South China University of Technology) was 1,850 $mmol \cdot g^{-1}$ at 3,405 kPa and 298 K. He et al. [127] conducted a study investigating the efficiency of benzene uptake in a diverse range of isoreticular MOFs, including NENU-511 to NENU-514 (NENU stands for Northeast Normal University) (Fig. 7a) by merging 4 bidentate chelators with varying quantities of methyl and phenyl groups with a 4,4′,4″-benzene-1,3,5-triyl-tri-benzoic acid ligand (H3BTB). The levels benzene adsorption of NENU-511-514 at 298 K are 1,556; 1,519; 1,687 and 1,311 $mg \cdot g^{-1}$, respectively (Fig. 7b) [128].

Huang et al. [129] have prepared a novel nanotubular Zn-MOF obtained from biphenyl-3,5-dicarboxylic acid. This

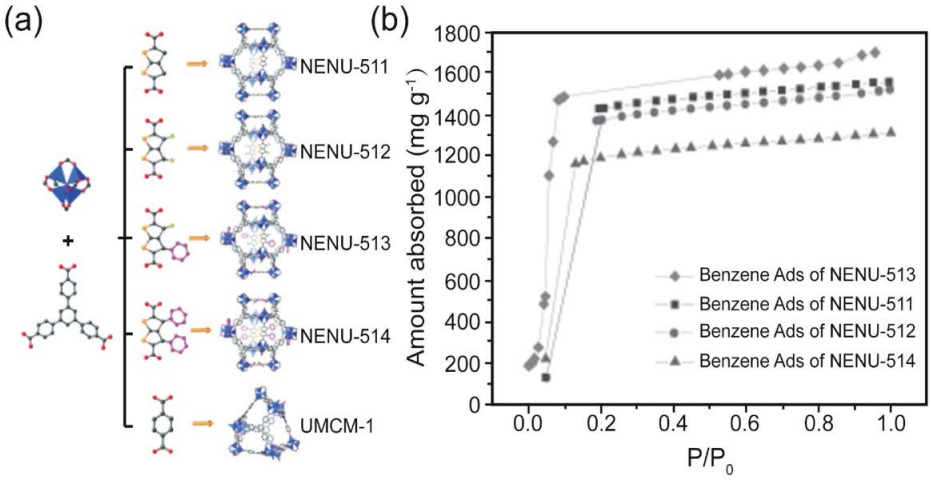

Fig. 7. (a) Structures and building blocks of NENU-511-514. (b) Benzene adsorption isotherms at 298 K for NENU-511-514. Reproduced with permission from John Wiley and Sons ref. [127] (License ID 5647820554538).

material is thermodynamically stable and exhibits excellent topological, structural and adsorbent characteristics. The measured values for p-xylene, m-xylene, and benzene were 1.79, 1.04, and 1.08 mg·g^{-1}, respectively. Adsorption competition was also investigated with liquid phase benzene/xylene and benzene/toluene. The nuclear magnetic resonance (NMR) research findings demonstrated Zn-MOF's effective distinction of benzene from xylene and toluene [129].

3.1.3. NO_2 removal

NO_2 is a commonly found hazardous pollutant and a prevalent chemical contaminant. Many sorbents containing MOF have been developed and tested in the past to remove NO_2. Among various MOFs reported, Zr(IV)-based MOFs have received extensive attention owing to their excellent chemical stability for NO_2 removal. Peterson et al. [130] conducted a study using UiO-66-NH_2 and found it to be effective in eliminating NO_2 from the air (Fig. 8). Additionally, they tested UiO-66 and BPL (Trademark owned by Calgon Corporation) activated carbon for comparison purposes. UiO-66-NH_2 demonstrated a NO_2 saturation capacity of 0.9 g·NO_2·g^{-1}. Moreover, at 80% relative humidity, the NO_2 loading capacity for UiO-66-NH_2 exceeded 1.4 g·NO_2·g^{-1}. This increase in exposure to UiO-66-NH_2 was ascribed to the higher water content at 80% relative humidity, which enabled the MOF to react with NO_2 more easily [130].

Ebrahim and Bandosz [131] analyzed MOF synthesis with NH_2 groups derived from the reported urea based on modified Zr(IV). In order to extract NO_2 from dry or humid air, the samples were used as adsorbents. Through the incorporation of NH_2 groups, the introduction of Lewis base sites promotes chemical reactions on the surfaces of MOFs. Additionally, water enhances the process of NO_2 adsorption. In both moist and arid conditions, the carbonyl (C=O) groups and amine (NH_2) groups in urea directly interact with NO_2 molecules, resulting in surface-bound nitrates being formed. In wet conditions, the NO_2 adsorption capacity of urea-modified UiO-66 was significantly enhanced, with an impressive adsorption rate of 101 mg·g_{ads}^{-1}, which is more than 100% higher compared to the standard UiO-66, which only adsorbs at a rate of 40 mg·g_{ads}^{-1}. This substantial improvement

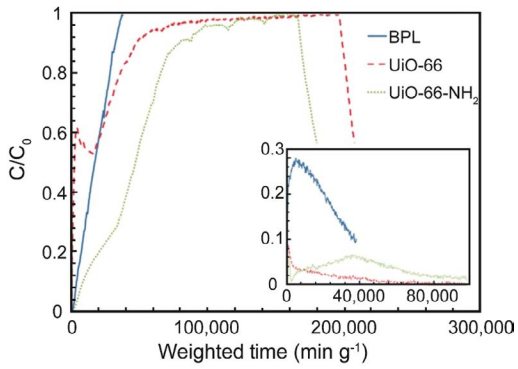

Fig. 8. Breakthrough curves of NO_2 for BPL, UiO-66, and UiO-66-NH_2 under dry relative humidity, with a NO elution inset. Reproduced with permission from John Wiley and Sons ref. [130] (License ID 5647820234421).

demonstrates the effectiveness of the urea modification in boosting the adsorption potential of UiO-66 under wet conditions.

Audu et al. [132] developed a method to remove NO_2 generated from the Solvent Assisted Ligand Incorporation (SALI) process of synthesizing a UiO-66 analogue, UiO-66-ox (ox-oxalic acid). UiO-66-ox has the potential to extract NO_2 more effectively than UiO-66 from the gas stream. The addition of oxalic acid resulted in a doubling of the adsorption potential of NO_2 to 8.4 mmol·g^{-1}, as compared to the 3.8 mmol·g^{-1} achieved by UiO-66. The rise is associated with SBU (secondary building units) or free carboxylic acid and is estimated to be ~6.3 NO_2 molecules for SBU. NO_2 removal which increases relates to the potential reactivity of the carboxylic with NO_2 [133].

3.1.4. SO_2 removal

The standard gases from the burning of coal dust include CO_2, SO_2 and NO_2. It is possible to extract much of the SO_2 by scrubbing and making it into salt. Traces of SO_2 in vapours, though, cannot be eliminated by such methods. During the process of CO_2 scrubbing, there is a potential issue with residual SO_2 present in the flue gas. This SO_2 can react with organic amines, leading to a permanent loss of amine activity and reducing the overall efficiency of the process. Therefore, it is crucial to completely eliminate SO_2 residues from the vapors. One promising approach for selective gas elimination is reversible physisorption using porous materials.

However, using MOFs as adsorbents for SO_2 removal has been challenging due to their inadequate stability against highly reactive SO_2, which has hindered the design of effective experiments [134]. Nevertheless, a series of MOFs, specifically M(bdc)$(ted)_{0.5}$ (M = Ni, Zn; bdc = 1,4-benzene dicarboxylate; ted = triethylenediamine), were reported by Tan et al. [135] for selective SO_2 adsorption. At room temperature and 1.13 bar, the adsorption of SO_2 in Ni(bdc)$(ted)_{0.5}$ was measured to be 9.97 mmol·g^{-1}. Theoretical simulations indicated two possible adsorption configurations for the adsorbed SO_2 molecules. In one configuration, the SO_2 molecule binds to the O atom of the paddle-wheel building unit through its S atom and its two O atoms to the C–H groups of hydrogen-bonding organic linkers. In the other configuration, SO_2 forms a hydrogen bond with the ted ligand group –CH_2, which is connected at the same time by its two O atoms.

At 298 K and 1 bar, the SO_2 adsorption capacity of MFM-300 (In) (Manchester Framework Material) was found to be 8.28 mmol·g^{-1} (Fig. 9a). In another study, Savage et al. [136] published the results of a MOF, MFM-300 (In), for selective SO_2 adsorption. The selectivity of MFM-300 (In) was measured for binary gas mixtures at 1 bar and 298 K, and it was found to be 5,000 mmol·g^{-1} for SO_2/N_2, 425 mmol·g^{-1} for SO_2/CH_4, and 60 mmol·g^{-1} for SO_2/CO_2, respectively (Fig. 9b).

Moreover, without degrading the structure, the substance may be regenerated. Further experiments have reported that adsorbed SO_2 molecules form unique several supramolecular associations on the pore surface of this material with free hydroxyl groups and aromatic rings, rationalizing the selectivity found at the molecular level.

Systematic investigation of SO_2 adsorption at atmospheric and low pressures on hexafluorosilicate SIFSIX-1-Cu,

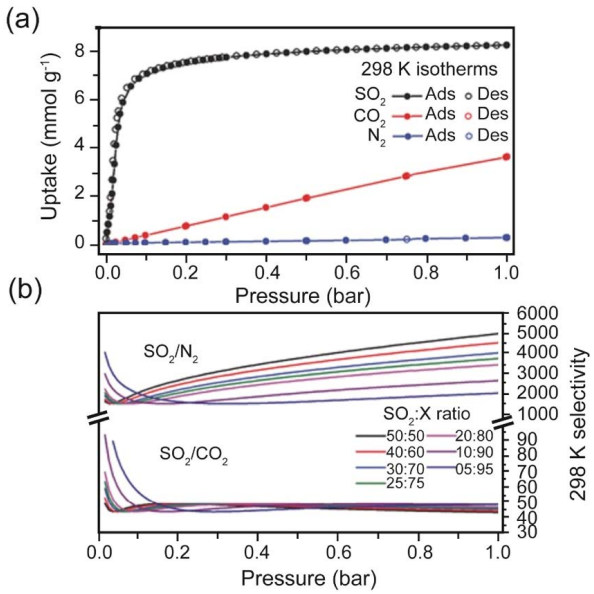

Fig. 9. (a) Adsorption isotherms of SO_2, CO_2 and N_2 (b) selectivity of MFM-300 (In) for SO_2/N_2 and SO_2/CO_2 mixtures is determined using the Ideal Adsorbed Solution Theory at 298 K and 1 bar. Reproduced with permission from John Wiley and Sons ref. [136] (Creative Commons CC BY license).

SIFSIX-2-Cu, SIFSIX-2-Cu-i, SIFSIX-3-Zn, and SIFSIX-3-Ni was carried out by Cui et al. [137]. In Fig. 10a, it is evident that SIFSIX-1-Cu outperforms the other SIFSIX compounds, displaying a higher SO_2 capacity of 11.01 mmol·g^{-1} at 298 K and 1.01 bar. Moving to Fig. 10b, we observe that SIFSIX-2-Cu-i exhibits remarkable SO_2 adsorption at an extremely low partial pressure (0.002 bar) and 298 K, with a value of 2.31 mmol·g^{-1}. However, when the partial pressure was raised to 0.01 bar, the SO_2 adsorption of SIFSIX-2-Cu-i increased to 4.16 mmol·g^{-1}. Further analysis in Fig. 10c shows that SIFSIX-2-Cu-i has an impressive SO_2/CO_2 selectivity ratio of 86–89 at a proportion of SO_2 ranging from 0.1 to 0.9 M. Finally, in Fig. 10d, we find that SIFSIX-1-Cu surpasses SIFSIX-2-Cu-i in terms of SO_2/N_2 separation selectivity, with values ranging from 2,510 to 3,145.

These results highlight the superior performance of SIFSIX-1-Cu in terms of SO_2 capacity, while SIFSIX-2-Cu-i demonstrates remarkable selectivity for SO_2 over CO_2 and N_2 under specific conditions [137].

3.1.5. Adsorption of fluorinated gases

Generally, the inclusion of fluorinated compounds is another class of gas pollutants that are considered highly detrimental to the environment. Chlorofluorocarbons (CFCs) pose a significant threat to the ozone layer in the stratosphere in particular. The incremental substitution of CFCs with other forms of service fluids in cooling processes has restored the functionality of the planetary natural UV shield substantially over the past decades. There are other classes of fluorinated gases that can be known to be particularly toxic to the atmosphere of the earth. Among them, halogenated general anesthesia gases (HGAGs) are an emerging threat due to their uncontrolled and globally released growth [138]. This is because even Cl-containing HGAGs (e.g., enflurane and isoflurane) are known as CFCs, whereas global warming potential is characterized by sevoflurane, desflurane, and isoflurane [139]. Among HGAG's realistic technologies for emission control, those guaranteed for adsorption are defined as the most effective. MOFs are currently being used in experiments on the adsorption of these gases. However, the adsorption properties of sevoflurane (SF) in MOF-177 were stated in the only article that discussed this issue and considered the use of a commercially available adsorbent [140]. The only MOF deemed suitable for the detection of HGAG is MIL-101, which is not currently available in large quantities as a potential product. MIL-101 has a higher SF adsorption capacity than a benchmark adsorbent generally used by HGAG. Unfortunately, as already expected, these technologically possible outcomes should not be the performance of HGAG scanning systems, which can be achieved in operating theatres at the moment, as there is no MIL-101 certainty to be produced commercially [141].

3.1.6. Adsorption of radioactive gases

Nuclear fission creates fission products, particularly those that are reactive under the conditions of reprocessing spent fuel and the production of medical isotopes. ^{129}I, ^{127}Xe and ^{85}Kr are the radionuclides listed as notable for separation during flue gas treatment [142]. Existing strategies of trapping I_2 by porous adsorbents include the use of silver-based zeolites. These materials lack high adsorption capabilities due to their comparatively small surfaces. Silver metal use also raises questions about the expense and effect on the environment [143]. A few experiments have been performed on the adsorption of I_2 by MOF, and the adsorption of I_2 is not especially high in these papers [144–146]. Because of its adequate pore capacity, large surface area, and high chemical and thermal stability, ZIF-8 was selected as a new I_2 adsorbent. It was observed that each cage was stuck with up to 5.4 I_2 molecules and that I_2 adsorption was mostly due to beneficial interactions with the ZIF-8 organic linker. The raised loads of I_2 resulted in decreased crystallinity, but the cages' connectivity was preserved as shown in Fig. 11 [147]. When extruded into granules, ZIF-8 maintained its high I_2 adsorption capability. The tiny pores of ZIF-8 will restrict I_2 loss after adsorption. This adsorption in ZIF-8 then allows I_2 to be separated and inserted into suitable types of waste [148].

The synthesis and characterization of a new ZIF, ZIF-mnIm, which has the same topology as ZIF-8, but with a different organic linker, has been documented by Bennett et al. [149]. The adsorption of I_2 in ZIF-mnIm was calculated and the efficiency was compared to that of known ZIF frames. They observed that, due to the large pore opening, ZIF-mnIm had the highest initial adsorption, but poor retention. It was also found that the retention temperature from I_2 to 100°C was greatly improved by mechanical grinding of filled samples. Although ZIF-8 was the overall best candidate for I_2 uptake and retention, the largest improvement in retention temperature after grinding was seen by ZIF-mnIm [149].

A major step in the isolation of toxic ^{127}Xe and ^{85}Kr from gaseous spent fuel reprocessing is the extraction of low

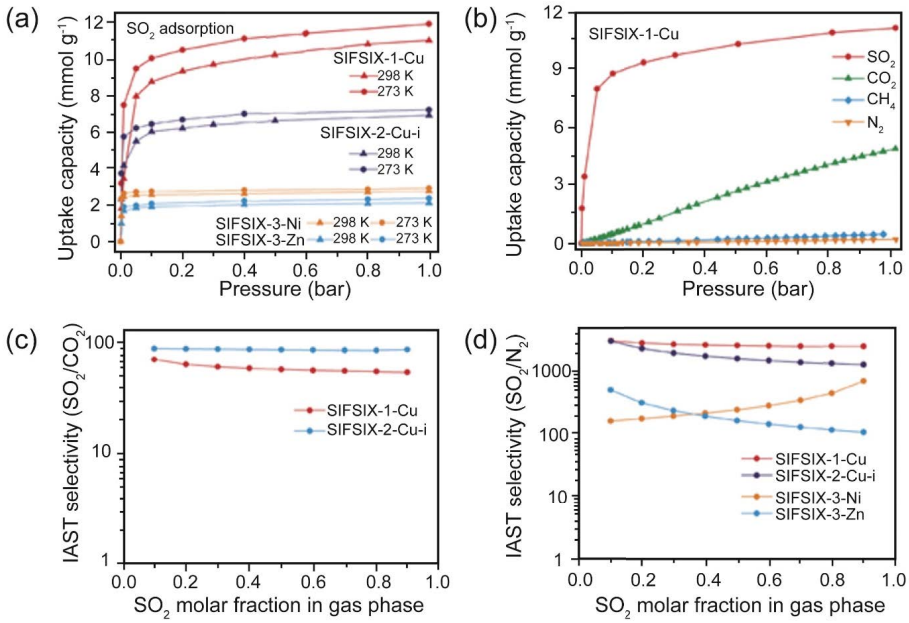

Fig. 10. (a) Adsorption isotherms of SO_2 on SIFSIX-1-Cu, SIFSIX-2-Cu-i, SIFSIX-3-Ni and SIFSIX-3-Zn are presented at temperatures of 273 and 298 K. (b) At a temperature of 298 K, the adsorption isotherms for SO_2, CO_2, CH_4, and N_2 on SIFSIX-1-Cu are provided. Additionally, the Ideal Adsorbed Solution Theory selectivities of SIFSIX materials are evaluated for (c) SO_2/CO_2 mixtures and (d) SO_2/N_2 mixtures, considering varying molar fractions of SO_2 in the gas phase at a pressure of 1 bar. Reproduced with permission from John Wiley and Sons ref. [137] (License ID 5647811275653).

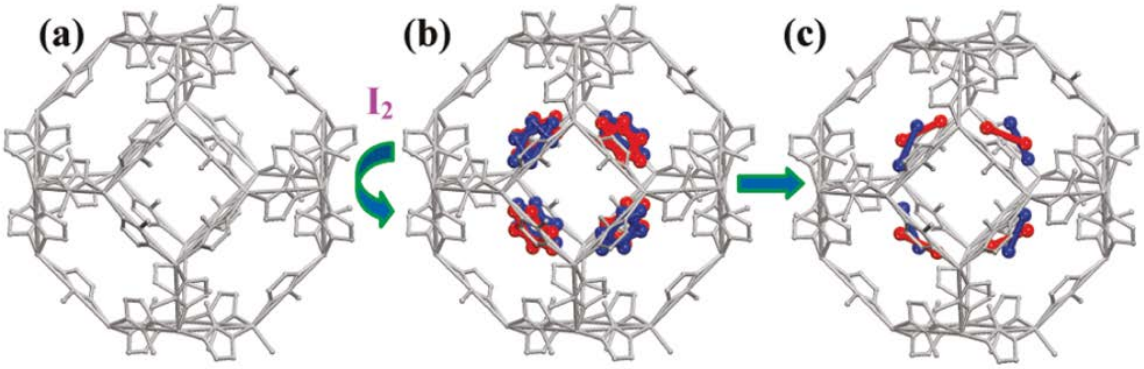

Fig. 11. Illustrates: (a) the ball-and-stick model of the activated cage before I_2 loading, (b) two refined molecular I_2 adsorption sites inside the β-cage labeled as "Ia" (blue) and "Ib" (red), and (c) the actual molecular arrangement with omitted hydrogen atoms for clarity. Reproduced with permission from ACS ref. [147] (License ID 1684275).

concentrations of Xe and Kr from the air. Cryogenic distillation, which requires a lot of electricity and can be pricey to install, is the current way of removing these toxic gases. Conversely, through selective adsorption, the isolation of Xe and Kr at room temperature may be more energy-efficient and less costly overall [150]. In some MOFs, noble gas storage has been reported, but research to date is very limited [151,152]. Thallapally et al. [153] have recently reported that Ni/DOBDC can adsorb 4.16 mol·Xe·kg^{-1} MOFs to 100 kPa and 298 K [153]. Besides, Liu et al. [154] used a column approach to analyze the low MOF concentration adsorption of Xe and Kr. For the first time, their experimental findings revealed that Ni/DOBDC could isolate 400 ppm Xe with an overall Xe/Kr selectivity of 7.3, from the 40 ppm Kr mixture in the air.

3.2. MOFs-based for capture of volatile organic compounds

For the trapping of volatile organic compounds, the properties of adsorbent materials can vary greatly from those of gases. In this respect, the diffusion kinetics of vapour molecules in narrow pore materials could be very slow and, from the other side, in the presence of humidity, the presence of open metal sites may sometimes be a drawback to the purification of air/gas. In the literature analysis, several selective adsorbents for volatile organic compounds such as tetrahydrothiophene, benzene, dichloromethane, and ethylene oxide are presented [155]. However, kinetic adsorption media, particularly MOF-5 and MOF-177, do not perform well in this regard. Surprisingly, IRMOF-62, largely substituted by BPL

carbon, is not as effective for certain vapours. Additionally, IRMOF-3 is found to be a bad adsorbent since none of them behaves like a strong Lewis acid, except in the case of ethylene oxide adsorption, where all products are similarly unsuccessful.

It has been shown that MOFs containing open metal sites are most efficient in extracting vapours from the gas stream. In the adsorption of ethylene oxide, BPL carbon is surpassed by an order of magnitude by Zn-CPO-27 and $[Cu_3(btc)_2]$. However, $[Cu_3(btc)_2]$ remains efficient, while Zn-CPO-27 shows limited effectiveness against the entire vapor spectrum. When adsorbing benzene and dichloromethane, $[Cu_3(btc)_2]$ demonstrates little difference in efficiency. However, it shows a remarkable increase in adsorption capacity compared to BPL carbon when capturing tetrahydrothiophene. Nevertheless, it is important to consider that the efficiency of $[Cu_3(btc)_2]$ can be significantly impacted by moisture, as water molecules may obstruct the unoccupied metal sites. MIL-101 ($[Cr_3F(H_2O)_2O(bdc)]$) effectively adsorbs a diverse range of VOCs with different polarities and functional groups, including acetone, benzene, toluene, ethylbenzene, xylenes, n-hexane, methanol butanone, dichloromethane, and n-butylamine. Huang et al. [156] demonstrated that MIL-101 exhibits a higher affinity for VOCs containing aromatic rings, particularly amines, and those with heteroatoms. Compared to commonly used adsorbents like resins, zeolites and activated carbon equivalents, MIL-101 demonstrates a superior propensity for adsorbing xylenes, toluene, acetone and ethylbenzene [157].

At a temperature of 288 K and a pressure of 56 mbar, MIL-101 demonstrates an adsorption capacity of 16.7 $mmol \cdot g^{-1}$ for benzene, which exceeds the values observed for zeolites (SBA-15 and Silicalit-1) by nearly two-fold and surpasses activated carbon (ACF and Ajax) by 3–5 times. Moreover, the desorption curve profile exhibits two distinct peaks, corresponding to the two major benzene adsorption points. Strong interactions would take place between the adsorbate molecules and the Cr^{3+} metal centers, while significantly weaker interactions would occur between the adsorbate and the pore space. It is evident from subsequent adsorption–desorption experiments that fast desorption kinetics, high desorption efficiency, and stable adsorption performance across five cycles can be achieved. The efficiency of benzene desorption may exceed 96%, which shows that benzene adsorption–desorption is extremely reversible [158]. In other words, when the material $[Cu_3(OH)(capz)]$ (where A can be NH^{4+}, Li^+, Na^+, K^+, Me_3NH^+, Et_3NH^+) is exposed to mixtures of benzene and cyclohexane vapours, significant enhancements occur in its porous surface composition and the adsorption selectivity for benzene-cyclohexane mixtures. This improvement is achieved through the exchange of NH^{4+} cations within the porous structure of the anionic MOF, $NH_4[Cu_3(OH)(capz)]$ (where capz stands for 4-carboxypyrazolate). This modification results in a considerable increase in the amount of benzene adsorbed during the process [159].

Xylene and ethylbenzene isomers are adsorbed by the compact MIL-53(Al) structure, showing two distinct phases and hysteresis in adsorption isotherms at 110°C due to the existence of adsorbent molecules, leading to the structure's opening. The sorption line narrows the arrangement at low pressures. A single group of molecules can be a group in a single file arrangement, which is adsorbed along the length of the pores, inside the enclosed confines of the MIL-53(Al) structure's closed shape. The pores are opened up again at even higher pressures [160]. There is ample space in the open form for xylene isomers to be adsorbed in pairs along the length of the pores, resulting in a doubling of the adsorbed volume (Fig. 12). Because of the differing efficiency with which the pores can be filled with differing isomers, the ability of adsorption is greatly affected. This effect is called proportional adsorption which happens when the adsorbate's size which molecular form results in an alignment and adsorbed sum that is aligned with the adsorbent's crystalline symmetry and pore structure and is self-consistent [161].

An updated MOF, MIL-47 (V), filled with $CuCl_2$, exhibits a remarkable benzothiophene adsorption ability. MIL-47(V) exhibits an unusual decreasing ability, it is probable that the existence of V(III) within the MOF contributes to the generation of Cu(I) ions from charged Cu(II) ions. The Cu(I) ions obtained, display an advantageous effect, presumably by π-complexation, on benzothiophene adsorption. $CuCl_2$ concentration has been shown to cause an increase in adsorption potential up to a certain magnitude ($Cu/V = 0.05\ mol \cdot mol^{-1}$). However, when the $CuCl_2$ load is further increased beyond the previously mentioned point, the adsorption potential starts to decrease. This is due to the acidity/porosity contribution of a Cu(I) site and MIL-47(V) originating from $CuCl_2$ [162]. The production of sensor materials, on the other hand, is also an area of research that is highly active. As shown in Fig. 13, $[Zn_2(bdc)_2$-(dpNDI)n] is a compound consisting of benzene-1,4-dicarboxylic acid (H_2bdc) and N, NO-di(4-pyridyl)-1,4,5,8-naphthalenediimide (dpNDI). It forms strong stacking interactions with VOC molecules. As a consequence, the emission color of the compound undergoes a significant shift, which is influenced by the ionization potential of each VOC molecule [163].

The {Fe(pyz)[Pt(CN)$_4$]} method can incorporate several vapor host molecules, such as CS_2 and benzene, altering the materials' optical, magnetic and pore size characteristics. This integration could potentially serve sensing purposes [164]. As previously stated, when exposed to environmental humidity, unsaturated coordinated metal site-based MOFs like $[Cu_3(btc)_2]$ are not effective in capturing (VOCs). A new versatile MOF, called [Ni(bpb)](H2bpb = 1,4-(4-bispyrazolyl) benzene), which is effective in adsorbing benzene and cyclohexane, is used to solve this problem [165]. Moreover, this substance effectively eliminates tetrahydrothiophene from CH_4-CO_2 mixtures, even in the presence of 60% humidity and dynamic conditions, surpassing the limitations of MOF-5 and $[Cu_3(btc)_2]$ in real-world applications. Finding efficient adsorbents for such hazardous substances is crucial in practical scenarios. It should be remembered that humidity is still present in actual environments and water molecules are a major competitor for the adsorption of these toxic molecules. The use of strongly hydrophobic MOFs to trap warfare agents in this sense is an adequate technique for the selective adsorption of these molecules even under conditions of extreme humidity. For instance, for capture of di-isopropyl fluorophosphate (DIFP, sarin nerve gas model) and diethyl sulfide (DES, mustard gas model bubbles), MOF-5 $[Zn_4O(dmcapz)3]$ (dmcapz = 3,5-dimethyl-4-carboxypyrazolate) is appropriate candidate [166].

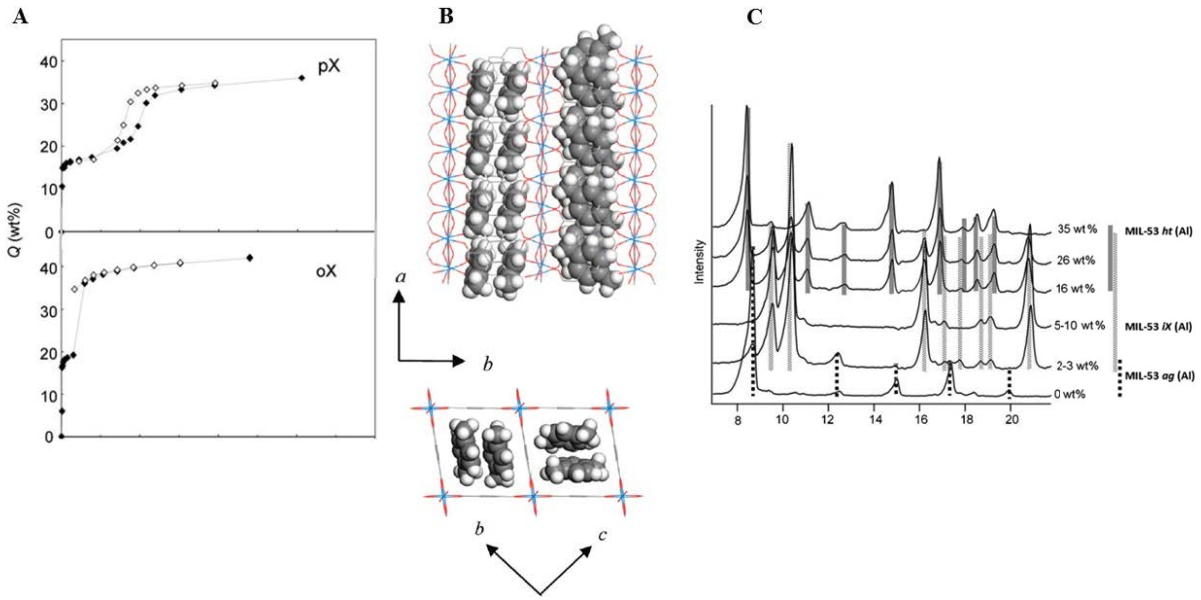

Fig. 12. (A) Isotherms for adsorption (represented by solid symbols) and desorption (represented by open symbols) of o-xylene (oX) and p-xylene (pX) at a temperature of 110°C are measured on MIL-53(Al). (B) Behavior of p-xylene at 110°C within the pores of MIL-53(Al). (C) X-ray diffractograms of MIL-53(Al) with varying loadings of o-xylene (oX). Reproduced with permission from John Wiley and Sons ref. [160,161] (License ID 5647810618673).

This compound exhibits remarkable stability in terms of its chemical, mechanical, and thermal properties, which is assured by the M-NO (carboxypyrazolate) coordination bond form. Furthermore, it is strongly hydrophobic, contributing to essential partition coefficients of VOC-H_2O. [$Zn_4O(dmcapz)_3$] outperforms [$Cu_3(btc)_2$] under atmospheric conditions, and does not maintain DIFP or DES upon hydration. The efficiency of [$Zn_4O(dmcapz)_3$], however, resembles that of activated carbon molecular sieve, implying related sorption mechanisms governed by the non-polar existence and small size of the pores in the two materials [166]. Research has shown that to optimize these porous materials for specific industrial uses, it is essential to enhance the stability of MOFs against ambient humidity. Consequently, pre- and post-synthetic modification methods have been investigated to improve the hydrophobicity of MOFs. The incorporation of alkane or fluoroalkane residues into organic linkers is one of the most promising methods [124]. The synthesis of completely fluorinated MOFs characterized by FMOF-1 and FMOF-2 from the combination of Ag^+ with 3,5-bis (trifluoromethyl)-1,2,4-triazolate was stated in this context by Yang et al. [167]. The hydrophobic nature of FMOF-1 is primarily due to the efficient selective adsorption potential observed for aliphatic and aromatic oils (benzene, toluene, p-xylene, cyclohexane and n-hexane) components that prevent water molecules from entering their pores [167]. In Fig. 14, the isoreticular MOFs such as [$Ni_8(OH)_4(H_2O)_2(L)_6$] (H_2L_1 = 1H-pyrazole-4-carboxylic acid; H_2L_2 = 4-(1H-pyrazol-4-yl) benzoic acid, H_2L_3 = 4, 4′-benzene-1,4-diylbis-(1H-pyrazole), H_2L_4 = 4,4′-buta-1,3-diyne-1,4-diylbis (1H-pyrazole), H_2L_5 = 4.4′-(benzene-1,4-diildietin-2,1-diyl) bis (1H-pyrazole), H_2L_5-R (R = methyl, trifluoromethyl)) shows that the use of metal azolate coordination bonds leads to more stable materials [124].

Furthermore, the pore size and surface polarity are influenced by the length and functionalization of linkers. In a very competitive humid environment (up to 80% relative humidity), the key data about the capture of harmful agents were obtained and compared to hydrophobic activated carbon. Indeed, the analysis of the adsorbate step following the DES (diethyl sulfide) adsorption process in wet streams with a relative humidity of 80% reveals that under these conditions, only [$Ni_8(OH)_4(H_2O)_2L_5$-$CF_3)_6$] and carbon active capture DES demonstrate that the sorption of DES into this MOF does not influence the existence of humidity. In very complicated environmental conditions, this isoreticular sequence may be seen as a first step towards the rational nature of MOFs for the identification of hazardous VOCs [124].

3.3. MOFs for removal of inorganic pollution

Over the past few years, there has been a notable increase in the exploration of MOFs for their potential application in water treatment. This chapter provides a comprehensive review that specifically outlines the ability of MOFs to effectively eliminate inorganic contaminants. The section categorizes inorganic pollutants into three distinct groups: cationic contaminants, metalloids, and anionic trace elements, each characterized by distinct mechanisms of removal.

3.3.1. Metalloids removal

3.3.1.1. Arsenic removal

Due to its toxic nature, the contamination of water with arsenic (As) is a major concern. The existence of arsenic in water has the potential to be hazardous for the well-being of both people and the natural surroundings. It is essential to detect arsenate arsenite [As(III)] and [As(V)] in the

given context. The thermodynamically stable state of arsenic is As(V) and it is commonly present in surface waters, whereas arsenic(III) is typically detected in underground water sources [168]. Due to arsenic(V) being the dominant and thermodynamically stable form of arsenic in surface waters, scientists have synthesized MOFs that are specifically engineered to effectively capture and remove arsenic(V). The MOF, FeBTC, includes, as a metal node, iron and, as an organic linker, 1,3,5-benzenetricarboxylic acid. Using NaOH and HCl, its adsorption efficiency was evaluated under various pH conditions. At an initial concentration of As(V) of 5 $mg \cdot L^{-1}$ at pH 4, the removal efficiency of As(V) by Fe-BTC exceeds 96%. This MOF demonstrates an effectiveness that is 37 times greater at extracting As(V) than Fe_2O_3 nanoparticles [169,170]. The structure of zeolite imidazolate 8 (ZIF-8) has shown significant sorption capabilities for arsenic, offering at neutral pH, a capacity of adsorption of 59.89 $mg \cdot g^{-1}$ for As(III) and 50.15 $mg \cdot g^{-1}$ for As(V). This suggests a strong potential for the removal of As(III) due to its higher sorption capability in comparison to As(V). As a result of the higher concentration of loading for As(III) compared to As(V), optimal adsorption potential is observed for As(III) in relation to As(V). Despite using the same concentrations of As(V) and As(III) for the analysis, the adsorption behavior was not identical. As a result, As(V) displays a (PC) of 0.90 $L \cdot g^{-1}$, whereas As(III) displays a higher amount of 1.90 $L \cdot g^{-1}$ for the partition coefficient. This suggests that ZIF-8 is more efficient in adsorbing As(III) compared to As(V) [119].

In aqueous media, MOF-808, has also been used to extract As(V). During the initial 30 min at pH = 4, there was rapid adsorption of the original As(V) concentration of 5 $mg \cdot L^{-1}$, resulting in a high removal efficiency of 95% for As(V). Weak van der Waals interactions have been proposed as the adsorption mechanism between arsenate and the Zr metal nodal surface sites in MOF-808 [171]. Over a pH range spanning from 1 to 10, the MOF UiO-66 has shown promising capabilities for adsorbing arsenic. The confirmed uptake process involves coordinating metal node hydroxyl (–OH) group and/or replacement of ligands from benzenedicarboxylic acid, as confirmed by Fourier-transform infrared spectroscopy and PXRD [172]. The thiolate derivative of UiO-66, known as UiO-66-$(SH)_2$, exhibits a unique dual system for effectively capturing both As(V) and As(III). The thiolated ligands selectively bind to arsenite species, whereas the MOF node associates with arsenate species. After 6 h, the adsorption capacity of UiO-66-$(SH)_2$ for arsenite and arsenate is 10 and 40 $mg \cdot g^{-1}$, respectively [132,172]. Fluctuating adsorption potential for As(V) is demonstrated by MIL-53(Fe), a distinct type of MOF. The metal ion in the node plays a crucial role in this behavior. MIL-53(Fe) exhibits a partition coefficient value of 1.07 $L \cdot g^{-1}$ and a sorption capacity of 20 $mg \cdot g^{-1}$. This can be attributed to the Lewis interactions between the metal ion present in MIL-53 and the anionic $H_2AsO_4^-$ [173].

3.3.1.2. Removal of antimony

Sb, a non-metal, is frequently employed in ceramics, glasses, alloys and flame retardants [174]. The increasing release of antimony into land and surface water, with subsequent atmospheric contamination, has become a growing concern worldwide. Due to the potential adverse effects of prolonged exposure to antimony on human health, the US Environmental Protection Agency (USEPA) has set the permissible antimony content in drinking water at 6 $mg \cdot L^{-1}$ [175]. Antimonite and antimonate are the most often found oxidation states of antimony. In water, under oxic conditions and pH values above 3, Sb(V) is the dominant species present [176]. The MOF NU-1000 (NU stands for Northwestern University) has been utilized for extracting Sb(V) from water in a pH range of 1–11, owing to its thermal, mechanical, and chemical stability [177,178]. NU-1000, a Zr-based MOF, demonstrates high removal potential of 260 $mg \cdot g^{-1}$ within 30–48 h. The material displays resilience when exposed to diverse aqueous conditions, and the analysis of differential pair distribution functions has unveiled the mechanism by which antimony binds [179]. NU-1000 has the capacity to adsorb approximately 287.88 $mg \cdot g^{-1}$ of antimonate and 136.97 $mg \cdot g^{-1}$ of antimonite [180]. NU-1000 with a partition coefficient of 0.83 $L \cdot g^{-1}$, shows better efficiency for Sb(V), while its performance for Sb(III) is poorer (PC value of 0.32 $L \cdot g^{-1}$), indicating its suitability for the elimination of Sb(V) [179].

Zr-based MOFs, known for their excellent thermal and chemical stability, have gained significant interest in recent scientific studies. Researchers have explored the addition of amino groups, such as in UiO-66, to improve the sorption ability of MOFs based on Zr [181]. UiO-66(NH_2), an updated version of UiO-66 with amino groups, exhibits a strong interaction force with Sb, making it highly effective in adsorbing both Sb(V) and Sb(III). UiO-66 demonstrates a lower efficacy in antimonite removal, approximately 22 $mg \cdot g^{-1}$, but significantly higher efficiency for antimonate. In contrast, UiO-66(NH_2) shows improved efficiency with 40 $mg \cdot g^{-1}$ for antimonate and 38 $mg \cdot g^{-1}$ for antimonite uptake [182]. With increasing temperature, the adsorption efficiency of both UiO-66 and UiO-66(NH_2) MOFs improves. UiO-66 exhibits a PC amount of 0.13 $L \cdot g^{-1}$ for Sb(III) extraction, whereas UiO-66(NH_2) displays a PC value of 0.21 $L \cdot g^{-1}$. As a result, the modified version of the MOF proves to be more effective for Sb(III) removal compared to its unmodified form [182].

3.3.2. Positively charged trace elements' removal

3.3.2.1. Mercury removal

Even in small amounts, mercury (Hg) is an highly poisonous metallic cation. It can be present in drinking water, and the World Health Organization (WHO) recommends a maximum concentration of 1 $mg \cdot L^{-1}$ for mercury in drinking water. Via food chain contamination, Mercury (Hg) has the tendency to bioaccumulate and can be transferred to humans. The toxicity or contamination of mercury predominantly impacts the victim's central nervous system. Cardiac disease, cardiovascular disease and even more are other biochemical consequences of Hg. For the reduction of toxic Hg cations, various forms of modified MOFs have been used [119]. During the initial 120-min contact with the polluted media, thiol-HKUST-1 exhibited an adsorption capacity exceeding 99%, effectively eliminating almost 716 $mg \cdot g^{-1}$ of Hg(II) from the media with an initial concentration of 415.5 $mg \cdot g^{-1}$ [183]. The introduction of a metal cluster containing iron enabled the magnetic modification of the simple

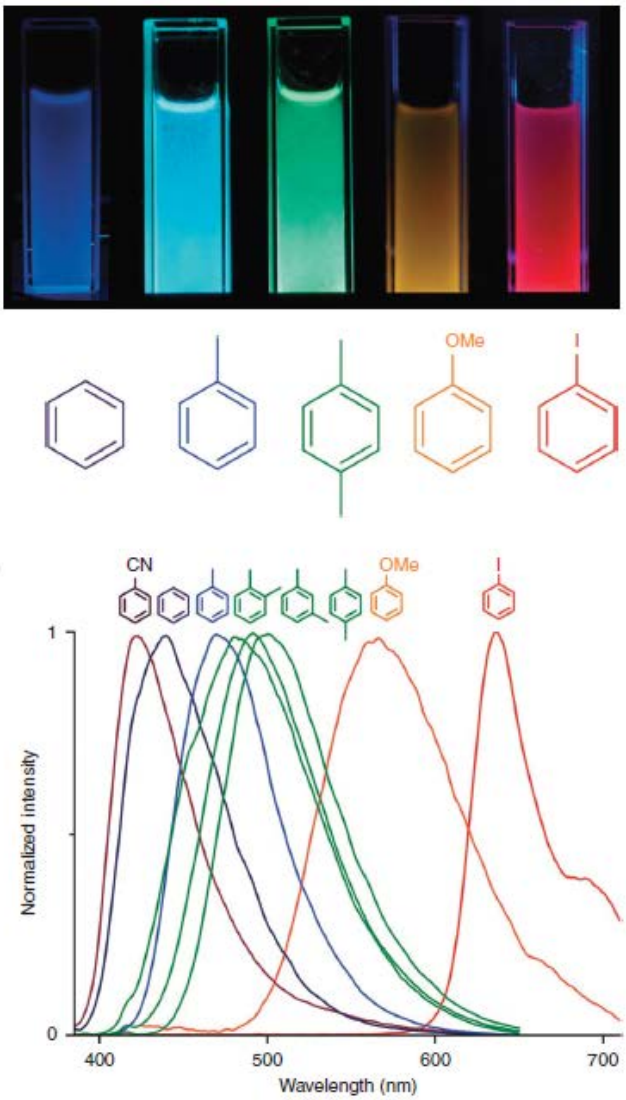

Fig. 13. Luminescence of the powdered $[Zn_2(bdc)_2(dpNDI)]_n$ material suspended in a liquid, exposed to different volatile organic compounds molecules after excitation at 365 nm using a commercial ultraviolet lamp. The bottom part of the figure presents the collected normalized spectra of the $[Zn_2(bdc)_2(dpNDI)]_n$@VOC compounds when excited at 370 nm. Reproduced with permission from Springer Nature, ref. [163] (under a Creative Commons license).

structure, resulting in (Fe_3O_4-SiO_2-HKUST-1). The highest Hg(II) uptake was observed at pH 3, reaching 265 mg·g^{-1} from an initial concentration of 21 mg·L^{-1}. Fe_3O_4-SiO_2-HKUST-1 and Thiol-HKUST-1 demonstrated relatively low partition coefficients of 1.30 and 0.50 L·g^{-1}, respectively [184].

UiO-66-NH_2 was subjected to post-synthetic modification through covalent modification to create UiO-66-NHC(S)NHMe MOF by Saleem et al. [185]. After 240 min from an initial concentration of 100 mg·L^{-1}, this new structure exhibited a Hg(II) adsorption capability of 99%. Modified UiO-66-NHC(S)NHMe exhibited a significantly higher adsorption capacity of 137.89 L·g^{-1} for Hg(II) compared to the efficiency of Zr-DMBD, which achieved complete uptake of Hg(II) from a starting concentration of 10.0 mg·L^{-1}. This comparison shows that the modified UiO-66-NHC(S)NHMe is a more efficient MOF for Hg(II) adsorption, considering its higher adsorption capacity [186].

Zn(hip)(L)(DMF)(H_2O), synthesized through solvothermal methods, demonstrated remarkable removal power for mercury. At a pH of 5, it showed the maximum potential for mercury removal, particularly at low concentrations such as 5, 10, and 20 mg·L^{-1}. The [Ni(3-bpd)$_2$(NCS)$_2$] MOF, as suggested by Halder et al. [187], exhibited Hg(II) adsorption with a color transition from green to grey. This MOF showed high selectivity for Hg compared to other solution ions for instance As^{3+}, Cd^{2+} and Pb^{2+}, resulting in a 95% uptake of Hg(II) from a 10 mg·L^{-1} solution. Numerous experiments have been conducted to evaluate the efficiency of different adsorbents in extracting Hg(II) ions from water, considering the high toxicity of mercury [187].

3.3.2.2. Removal of cadmium and lead

Cadmium (Cd) is a metal ion that can cause high levels of toxicity, mainly impacting vital organs like the liver and kidneys. On the other hand, lead(II) is known for its adverse neurotoxic effects. It bioaccumulates in food chains and poses particular toxicity risks to higher-order organisms within the food chain. The presence of radioactive metal ions like Cd and Pb in water bodies can lead to water contamination, which can have harmful consequences for marine organisms and humans [188]. To ensure the safety of drinking water and food supplies, the removal of these metals from water bodies is crucial.

Magnetic matrix composites for Pb(II) removal were developed by Ricco et al. [189] using a mixture of MIL-53 MOFs and nanoparticles of iron oxide. The incorporation of 50% amino-functionalized groups into the MOF of MIL-53(Al@100aBDC) resulted in a significant improvement in the adsorption of Pb(II), achieving a utmost reported capacity of 490 mg·g^{-1} in a 6-h period. Another highly efficient Pb(II) adsorbent in aqueous media is the MnO_2-MOF system, which demonstrated a remarkable adsorption potential of 917 mg·g^{-1} within 1 h. The pH of the solution decreased to 5 due to the release of protons during the adsorption process. Simultaneously, MnO_2-MOF exhibited encouraging prospects for the removal of Cd(II) [77].

In their study, Zhang et al. [190] established HS-mSi@MOF-5, a modified version of MOF-5 with a silica coating and thiol functionalization. At an optimal pH of 6, this novel material reached a capacity of 312 mg·g^{-1} for Pb(II) removal within just 30 min. In comparison, MOF-5 demonstrated a reasonable potential for removing Pb(II) at pH 4 and pH 6, but its efficiency decreased at pH 5. These variations in efficiency with changes in pH are attributed to the existence of acidic and basic active sites within the framework of MOF-5. The original MOF-5 without any alterations demonstrated a peak adsorption capability of 212 mg·g^{-1} for Pb(II) ions [191]. The performances of both MOFs in removing Pb(II) were excellent, with respective PC values of 7.0 and 7.6 L·g^{-1}. However, At pH 5, the reason for the reduced Pb(II) adsorption remains uncertain when compared to pH 4 and pH 6, considering the MOF-5 structure contains both acidic and basic active sites, which contribute to its versatile adsorption properties.

The Cd(II) adsorption potential of MOF-5 was lower, measuring at 3.60 mg·g^{-1}, with a slightly lower PC value of 0.01 L·g^{-1}. In contrast, the modified MOF showed a relatively higher PC amount of 2.61 L·g^{-1} for the removal of Cd(II). Moreover, HS-mSi@MOF-5 demonstrated a comparable equilibrium time of 30 min for Cd(II) adsorption when compared to Pb(II). However, its adsorption capacity for Cd(II) was lower at 98.0 mg·g^{-1} compared to Pb(II) [191].

Adsorptions for both Pb(II) and Cd(II) showed a similar equilibrium time and optimal pH, with TMU-5 exhibiting a removal capacity of 43 mg·g^{-1} for Cd(II) and 250 mg·g^{-1} for Pb(II).

In a span of 10 min, HKUST-1 MW@$H_3PW_{12}O_{40}$, which is derived from the MOF HKUST-1, exhibited a Cd(II) adsorption capacity of 32 mg·g^{-1} through chemisorption. Afterward, within 80 min, the material showed a Pb(II) uptake potential of 98 mg·g^{-1} [192].

At an optimal pH of 7 and during a 120-min timeframe, Cu-terephthalate MOF demonstrated an adsorption capacity of 90 mg·g^{-1} for Cd(II) and 80 mg·g^{-1} for Pb(II), with corresponding PC values of 2.51 and 2.28 L·g^{-1}, respectively [193]. Furthermore, compared to graphene oxide and zeolite, Cu-terephthalate MOF demonstrated outstanding adsorption capacity for the treatment of high acid drainage concentrations containing Mn, Cu, Zn, Fe, Cd, and Pb [194].

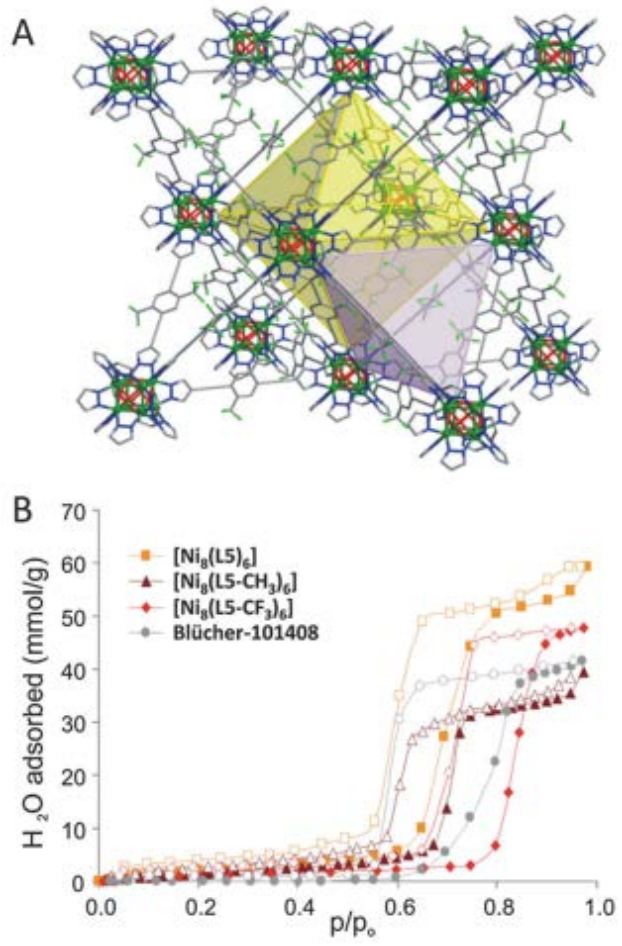

Fig. 14. (A) Crystal structure of the highly hydrophobic $[Ni_8(OH)_4(H_2O)_2(L_5)_6]$ compound, where H_2L_5 is defined as 4,40-(benzene-2,5-trifluoromethyl-1,4-diyldiethyne-2,1-diyl) bis-1H-pyrazole. (B) Effect of incorporating hydrophobic residues into benzene on the water adsorption isotherms at 298 K. Reproduced with permission from John Wiley and Sons ref. [124] (License ID 5647800443117).

3.3.3. Negatively charged trace elements' removal

3.3.3.1. Chromium removal

An element of industrial relevance is chromium (Cr), which has been discharged into the atmosphere in significant quantities. The two primary toxic forms of chromium are trivalent chromium (Cr(III) and hexavalent chromium (Cr(VI)). Cr(VI) is extremely hazardous and poses considerable risks to living organisms due to its carcinogenic and mutagenic properties. The main contributors to the atmospheric release of Cr(VI) ions are industries like leather tanning, pigment production, and dyeing processes.

Within a 2-h timeframe, a magnetic MOF named Fe_3O_4@MIL-100Fe was explored for its efficacy in eliminating hexavalent chromium. At an optimal pH of 2, this magnetic MOF demonstrated an impressive maximum sorption capability of ~19 mg·g^{-1}, achieving a partition coefficient of 0.175 L·g^{-1} [195]. At a pH of 10, TMU-5 functionalized with azine demonstrated an ultimate removal potential of 124 mg·g^{-1} [192]. In 10 min, an effective sorption capacity of 146 mg·g^{-1} was exhibited by TMU-30, besides a magnetized MOF, Fe_3O_4@MIL-100Fe, demonstrated a comparatively strong output of 2.05 L·g^{-1} within the same time frame [196].

The modified version of UiO-66, known as chitosan-MOF composite, displayed a robust electrostatic attraction between –NH_2 groups in the linkers and high oxidation state metal ions. This led to an impressive adsorption potential of 94 mg·g^{-1} for Cr(VI), with an exceptionally high PC value of 50.0 L·g^{-1} [197]. In terms of adsorption performance, the chitosan-MOF composite outperformed MOR-1-HA, a similar amino-functionalized MOF developed by Rapti et al. [198] which had a PC value of 0.32 L·g^{-1} and a maximum adsorption potential of 280.0 mg·g^{-1}.

3.3.3.2. Removal of fluoride

The global public health concern of removing fluoride from water supplies is an urgent issue [199]. Dental and skeletal fluorosis can occur as a result of prolonged consumption of water with fluoride levels exceeding 1.5 mg·L^{-1} [200]. Therefore, reducing fluoride levels in water sources is crucial for addressing these issues.

The investigation revealed that $[Ce(L_1)_{0.5}(NO_3)(H_2O)_2]$·2DMF exhibited significantly higher fluoride adsorption capacity (104.01 mg·g^{-1}) and a faster rate of fluoride uptake (1.80 g·mg^{-1}·min^{-1}) compared to its counterpart, $Eu_3(L_2)_2(OH)(DMF)_{0.22}(H_2O)_{5.78}$ [199]. Interestingly, the efficiency of the fluoride MOF decreased with increasing temperature. At 318 and 298 K, $[Ce(L_1)_{0.5}(NO_3)(H_2O)_2]$·2DMF showed PC values of 0.80 and 0.45 L·g^{-1}, respectively, outperforming $Eu_3(L_2)_2(OH)(DMF)_{0.22}(H_2O)_{5.78}$, which demonstrated PC values of 0.27 and 0.18 L·g^{-1} at 318 and 298 K, respectively. Another MOF called MIL-96(Al) was used for defluoridation

and demonstrated a maximum adsorption capacity of 31.69 mg·g^{-1}. At temperatures of 298, 308, and 318 K, MIL-96(Al) exhibited PC values of 0.96, 1.12, and 1.88 L·g^{-1}, respectively. Notably, higher temperatures resulted in improved fluoride adsorption efficiency [201].

At temperatures of 293, 313, and 333 K, the UiO-66-NH_2 system exhibited maximum adsorption potentials of 60, 53, and 42 mg·g^{-1}, respectively. The efficiency data for both MIL-96(Al) and UiO-66-NH_2 demonstrated an upward trend as the temperatures increased [202]. MOF-801, a fumarate-based MOF, achieved over 80% fluoride removal (32.13 mg·g^{-1}) with sorption efficiency of 0.25 L·g^{-1}. This non-toxic calcium fumarate (CaFu) MOF demonstrated an estimated overall fluoride uptake potential at 373 K of up to 166 mg·g^{-1} [203]. At 303 K, MOF-801 also displayed a sorption capacity of 40.1 mg·g^{-1}. It maintained strong and stable adsorption efficiency within the pH range of 2–10, even in the presence of high ion concentrations and other anions such as Cl, NO_3, and SO_4^{2-}. The adsorption efficiency was observed to increase with rising temperature. MOF-801 showed PC values of 0.4 L·g^{-1} at 293 K and 0.45 L·g^{-1} at 323 K. Within MOF-801, chemisorption is employed as an effective approach for defluoridation, involving the exchange of hydroxyl groups and fluoride ions [204].

3.3.4. Various ions sorption by MOFs

3.3.4.1. Phosphorous removal

Excessive phosphorus levels in surface water contribute to eutrophication, prompting environmental scientists to focus on its removal from aqueous media. In a recent study, a highly effective phosphate adsorbent, La-MOF, featuring a hierarchical structure composed of microspheres, nanorods, and nanoparticles, demonstrated remarkable adsorption capabilities, surpassing 170 mg·phosphates/g. La-MOF demonstrated a remarkable efficiency with a value of 4.03 L·g^{-1} [205]. Another water-stable MOF, zeolitic imidazolate system (ZIF-67), has shown effectiveness as a phosphate removal material. Optimum model parameters led to the highest PO_4^{3-} removal of 99.2%, achieved with a ZIF-67 dosage of 832.4 mg·L^{-1} at pH 6.82 and a mixing time of 39.95 min. Additionally, the maximum adsorption capacity for monolayer phosphate reached 92.43 mg·g^{-1}, while the thermodynamic properties indicated characteristics of random, physisorption, and endothermic processes [206]. Modified MOFs have been employed for phosphate adsorption to enhance removal capacity. At ambient temperature, the introduction of polyethyleneimine (PEI) into MOF UiO-66, with a PEI loading of 9.45%, resulted in an impressive maximum removal capacity of 73.15 mg of phosphorus per gram. This removal efficiency was maintained over a broad pH range, from 2 to 7, and reached equilibrium within a short timeframe of 50 min. UiO-66 impregnated with polyethyleneimine also demonstrated high regeneration efficiency, with more than six cyclic runs [207]. MIL-101, denoted as MIL-101@Zr(DS), was functionalized with ZrO_2 nanoparticles, resulting in a moderate PO_4^{3-} removal capacity of 22 mg·P·g^{-1} and an uptake efficiency of 0.24 L·g^{-1}. The inclusion of humic acid had a substantial impact on the adsorption potential of PO_4^{3-} within the MOF, leading to a reduction of two to ten times in adsorption, contingent upon the nanoparticles' dispersion [208]. UiO-66, a Zr-based MOF synthesized through solvothermal methods, displayed a phosphate adsorption capacity of 415 mg·g^{-1}, slightly surpassing other Zr-based adsorbents. This superiority is attributed to the strong attraction between PO_4^{3-} and Zr-OH groups. By introducing amino-substituted UiO-66-NH_2, the affinity for PO_4^{3-} was further enhanced through amine-PO_4^{3-} interactions, leading to a doubling of the removal potential with increasing temperature. Notably, both UiO-66 and UiO-66-NH_2 achieved complete removal (100%) of PO_4^{3-} from urine and diluted urine solutions [209].

3.3.4.2. Removal of radioactive metal ions

MOFs have shown great potential as adsorbents for the removal of radioactive metal ions, although the focus on this application is not as extensive as for other pollutants. Uranium U(VI) has received the most attention in the context of MOF-based removal. A wide range of MOFs had been tested for U(VI) sorption, with reported removal capacities ranging from 100 to 781 mg·g^{-1} [210]. The processes involved in removal of U(VI) primarily include ion exchange, carboxylic and amine coordination, electrostatic interactions, chemisorption and hydrogen bonding [211]. Pristine (e.g., MOF-2), modified (e.g., MOF-74), and composite (e.g., GO-COOH/UiO66) MOFs have been investigated for U(VI) adsorption. HKUST-1 demonstrated the highest uranium removal capacity, reaching 788 mg·g^{-1} at pH 6 and 60 min, with a PC value of 2.7 L·g^{-1}. Other MOFs, such as UiO-66-$(COOH)_2$, HKUST-1@$H_3PW_{12}O_{40}$ and SCU-100, exhibited maximum adsorption potentials of 540 mg·g^{-1} for ReO^{4-}, 350 mg·g^{-1} for Th^{4+}, and 350 mg·g^{-1} for Eu^{3+}, respectively [75]. SCU-100 MOF demonstrated considerable potential as an adsorbent, as indicated by its PC value of 1.82 L·g^{-1} for ReO^{4-} adsorption. The presence of Ag-O-Re bonds in the SCU-100 structure effectively trapped ReO^{4-} ions within its void spaces, highlighting its exceptional selectivity for ReO^{4-}. In comparison, UiO-66-$(COOH)_2$, a modified MOF, exhibited the highest PC value of 2.7 L·g^{-1} for Th^{4+} adsorption, while UiO-66-COOH and UiO-66 displayed lower PC values of 0.9 and 0.08 L·g^{-1}, respectively. The arrangement of carboxyl groups played a critical role in influencing the Th^{4+} adsorption efficiency of these MOFs [212].

The key factors affecting the adsorption of MOFs-based materials can be summarized:

(1) ***MOF composition***: The choice of metal ions and organic linkers in the MOF structure significantly influences its adsorption capabilities. Tailoring these components can enhance adsorption efficiency.
(2) ***Pore structure and surface area***: MOFs offer high surface area and tunable porosity. This parameter greatly impacts their adsorption potential, as it provides more active sites for contaminant binding.
(3) ***Stability and water resistance***: MOFs are generally not stable in water, which is a challenge for real-world applications. Researchers have developed thermally and water-stable MOFs to overcome this limitation.
(4) ***Specific contaminant targeting***: MOFs can be designed to selectively adsorb specific contaminants by matching their chemical properties. This selectivity is vital for efficient pollutant removal.

(5) ***Composite materials***: Combining MOFs with other adsorbents or materials can enhance their overall adsorption performance and address specific pollutant removal challenges.

Moreover, it is essential to understand the mechanisms behind MOF-based adsorption for a more comprehensive view:

(1) ***Host-guest interactions***: MOFs often utilize their porous structures to capture and hold pollutant molecules through host-guest interactions. Contaminants are physically adsorbed within the MOF pores, relying on factors like pore size and shape to determine which pollutants can be effectively adsorbed.
(2) ***Chemical bonding***: In some cases, MOFs form chemical bonds with pollutants. This can involve coordination bonds, covalent bonds, or other chemical interactions. For example, inorganic pollutants like metal ions can form coordination bonds with metal sites in the MOF structure.
(3) ***Surface adsorption***: MOFs may also adsorb pollutants on their external surfaces, especially when the pore structure is not suitable for accommodating the contaminants. Surface adsorption typically relies on physical interactions, such as van der Waals forces or electrostatic interactions.
(4) ***Tunable selectivity***: MOFs can be designed with specific functional groups or tailored structures that enable selective adsorption based on the chemical properties of the contaminants. This tunable selectivity is a critical mechanism in addressing various pollutants.
(5) ***Competitive adsorption***: Competitive adsorption occurs when multiple types of pollutants are present. MOFs may exhibit preferences for certain pollutants, and this competitive behavior can be understood through the study of adsorption isotherms and kinetics.

By considering both the key factors and mechanisms, researchers can optimize the design and application of MOFs for effective environmental pollutant removal.

3.4. MOFs recyclability

MOFs have been shown to be highly recyclable and reusable in various applications. Das and Nagaraja [213] conducted a recent study demonstrating the creation of a highly efficient and recyclable catalyst for converting CO_2 into oxazolidinones. They utilized an N-heterocyclic carbene (NHC)-based MOF with embedded Cu(I), showcasing excellent recyclability and selective CO_2 uptake properties. This MOF's unique features, including a high density of CO_2-attracting NHC and catalytic Cu(I) sites within its 1D channels, enabled efficient CO_2 conversion into α-alkylidene cyclic carbonates and oxazolidinones under room temperature and atmospheric pressure conditions. Notably, the Cu(I)@NHC-MOF exhibited impressive recyclability over ten regeneration cycles, maintaining both catalytic activity and chemical stability.

Wen et al. [214] conducted a study describing the creation of a novel MOF-based photocatalyst designed for both gaseous pollutant degradation and adsorbent regeneration. This photocatalyst exhibited outstanding performance under visible light and demonstrated high stability and reusability. While MOFs are known to have relatively low stability due to weaker coordination bonds compared to materials like zeolites or porous carbon-based substances, they excel in CO_2 adsorption capabilities. Ding et al. [215] are actively working on enhancing the stability of MOFs. They summarize recent advancements in designing and synthesizing stable MOFs and MOF-based materials through de novo synthesis and post-synthetic structural processing. Their work emphasizes the importance of strategies to bolster MOF stability, which would expand their practical applications, especially in the context of CO_2 capture and conversion processes.

Several methods have been suggested for the recycling of MOFs. Firstly, solvent-based recovery is a common approach involving the dissolution of MOFs in suitable solvents, with the recovered MOFs being redeposited on various substrates. Horcajada et al. [216] and Zhu et al. [217] have showcased the feasibility of this method. Secondly, thermal decomposition can be employed to break down MOFs, leaving behind metal or metal oxide residues that can be reused for MOF synthesis, as investigated by Li et al. [218] and Furukawa et al. [219]. Thirdly, mechanical methods, including ball milling, can be utilized to break down MOFs, reducing the need for solvents, as exemplified by Xu et al. [220]. However, MOF recycling is not without challenges. Maintaining the structural integrity of MOFs during the recycling process, as highlighted by Furukawa et al. [219], is one concern. Contaminants within MOFs can impede recycling and may require purification steps, as seen in the work of Xu et al. [221].

Some recycling methods, such as thermal decomposition, can be energy-intensive, emphasizing the importance of developing more energy-efficient recycling processes, as pointed out by Li et al. [218]. Finally, a proactive approach involves the green synthesis of MOFs with reduced environmental impact to enhance their recyclability, which has been advocated by the study of Kumar et al. [222]. Addressing these challenges is essential for improving the sustainability of MOF recycling.

4. Conclusions and future perspectives

MOFs have emerged as promising adsorbents for the removal of toxic contaminants from wastewater. Extensive research has been conducted on using MOFs for the aqueous phase removal of environmental pollutants, highlighting their superior adsorption potential and kinetics compared to traditional adsorbents like AC and zeolite. The exceptional textural characteristics of MOF, including tunable porosity and large surface area, coupled with their ability for flexible incorporation, contribute to their enhanced adsorption performance. Various interactions such as π–π, electrostatic, acid–base, hydrogen bonding, and coordination with coordinatively unsaturated sites (CUSs) facilitate effective adsorption of pollutants onto MOFs. The specific interaction mechanisms depend on the nature of the pollutants and the structure/chemistry of the MOF. By carefully selecting metal ions and organic linkers during synthesis or through

post-synthetic modifications (PSMs), MOFs can be tailored to exhibit desired functionalities for specific applications. The synthesis approach employed for MOFs influences factors such as surface area, morphology, pore size, dimensionality, and chemical environment. Despite the promising potential of MOFs for water purification, several challenges need to be addressed. These include the durability of MOFs in aqueous environments, the recyclability and reusability of MOF materials, and their performance in treating complex wastewater effluents containing multiple pollutants. Further research is required to enhance our understanding of the adsorbate-MOF interactions and improve the adsorption capabilities of existing MOFs, as well as develop new MOFs. Water-stable MOFs are particularly sought after, and efforts should be made to introduce water resistance into MOF structures. Until water-stable MOFs are achieved, they can still serve as super adsorbents for wastewater treatment, particularly in point-of-entry (POE) and point-of-use (POU) water treatment systems for small-scale industries and individual households. Systematic studies on the structural adaptations of ligands in water environments are also needed. To promote the widespread applicability of MOFs, research efforts should focus on designing efficient and cost-effective synthesis processes, developing regeneration and recycling protocols, and exploring sustainable disposal options for spent MOF materials. The continuous evolution of MOFs towards improved efficiency and stability is crucial to establish them as widely accepted adsorbents in water purification, aligning with various safety and environmental standards.

References

[1] M. Puri, K. Gandhi, M.S. Kumar, Emerging environmental contaminants: a global perspective on policies and regulations, J. Environ. Manage., 332 (2023) 117344, doi: 10.1016/j.jenvman.2023.117344.

[2] U. Pöschl, M. Shiraiwa, Multiphase chemistry at the atmosphere–biosphere interface influencing climate and public health in the anthropocene, Chem. Rev., 115 (2015) 4440–4475.

[3] M. Kampa, E. Castanas, Human health effects of air pollution, Environ. Pollut., 151 (2008) 362–367.

[4] Z. Zhang, J. Chen, Y. Gao, Z. Ao, G. Li, T. An, Y. Hu, Y. Li, A coupled technique to eliminate overall nonpolar and polar volatile organic compounds from paint production industry, J. Cleaner Prod., 185 (2018) 266–274.

[5] J. Tang, T. An, J. Xiong, G. Li, The evolution of pollution profile and health risk assessment for three groups SVOCs pollutants along with Beijiang River, China, Environ. Geochem. Health, 39 (2017) 1487–1499.

[6] H.K. Okoro, J.O. Ige, O.A. Iyiola, J.C. Ngila, Fractionation profile, mobility patterns and correlations of heavy metals in estuary sediments from olonkoro river, in tede catchment of western region, Nigeria, Environ. Nanotechnol. Monit. Manage., 8 (2017) 53–62.

[7] A. Daripa, L.C. Malav, D.K. Yadav, S. Chattaraj, Chapter 7 - Metal Contamination in Water Resources Due to Various Anthropogenic Activities, S.K. Shukla, S. Kumar, S. Madhav, P.K. Mishra, Eds., Metals in Water: Global Sources, Significance, and Treatment Advances in Environmental Pollution Research, Elsevier, Amsterdam, 2023, pp. 111–127.

[8] J.L. Adgate, B.D. Goldstein, L.M. McKenzie, Potential public health hazards, exposures and health effects from unconventional natural gas development, Environ. Sci. Technol., 48 (2014) 8307–8320.

[9] L.F. Liotta, Catalytic oxidation of volatile organic compounds on supported noble metals, Appl. Catal., B, 100 (2010) 403–412.

[10] G.-L. Wei, X.-L. Liang, D.-Q. Li, M.-N. Zhuo, S.-Y. Zhang, Q.-X. Huang, Y.-S. Liao, Z.-Y. Xie, T.-L. Guo, Z.-J. Yuan, Occurrence, fate and ecological risk of chlorinated paraffins in Asia: a review, Environ. Int., 92–93 (2016) 373–387.

[11] M.A. Bari, W.B. Kindzierski, Ambient volatile organic compounds (VOCs) in communities of the Athabasca oil sands region: sources and screening health risk assessment, Environ. Pollut., 235 (2018) 602–614.

[12] S. Mentese, D. Tasdibi, Assessment of residential exposure to volatile organic compounds (VOCs) and carbon dioxide (CO_2), Global Nest J., 19 (2017) 726–732.

[13] Z. Guo, R. Ma, G. Li, Degradation of phenol by nanomaterial TiO_2 in wastewater, Chem. Eng. J., 119 (2006) 55–59.

[14] J. Chen, Z. He, G. Li, T. An, H. Shi, Y. Li, Visible-light-enhanced photothermocatalytic activity of ABO_3-type perovskites for the decontamination of gaseous styrene, Appl. Catal., B, 209 (2017) 146–154.

[15] M. Yao, Y. Ji, H. Wang, Z. Ao, G. Li, T. An, Adsorption mechanisms of typical carbonyl-containing volatile organic compounds on anatase TiO_2 (001) surface: a DFT investigation, J. Phys. Chem. C, 121 (2017) 13717–13722.

[16] C.A. Martínez-Huitle, S. Ferro, Electrochemical oxidation of organic pollutants for the wastewater treatment: direct and indirect processes, Chem. Soc. Rev., 35 (2006) 1324–1340.

[17] B. Ramesh, A. Saravanan, P. Senthil Kumar, P.R. Yaashikaa, P. Thamarai, A. Shaji, G. Rangasamy, A review on algae biosorption for the removal of hazardous pollutants from wastewater: limiting factors, prospects and recommendations, Environ. Pollut., 327 (2023) 121572, doi: 10.1016/j.envpol.2023.121572.

[18] H. Chen, C.E. Nanayakkara, V.H. Grassian, Titanium dioxide photocatalysis in atmospheric chemistry, Chem. Rev., 112 (2012) 5919–5948.

[19] S. Wu, X. Nie, Z. Wang, Z. Yu, F. Huang, Magnetron sputtering engineering of typha-like carbon nanofiber interlayer integrating brush filter and chemical adsorption for Li–S batteries, Carbon N. Y., 201 (2023) 285–294.

[20] E. Barea, C. Montoro, J.A.R. Navarro, Toxic gas removal-metal–organic frameworks for the capture and degradation of toxic gases and vapours, Chem. Soc. Rev., 43 (2014) 5419–5430.

[21] N.A. Khan, Z. Hasan, S.H. Jhung, Adsorptive removal of hazardous materials using metal–organic frameworks (MOFs): a review, J. Hazard. Mater., 244–245 (2013) 444–456.

[22] R. Matsuda, R. Kitaura, S. Kitagawa, Y. Kubota, T.C. Kobayashi, S. Horike, M. Takata, Guest Shape-responsive fitting of porous coordination polymer with shrinkable framework, J. Am. Chem. Soc., 126 (2004) 14063–14070.

[23] W. Huang, Y. Zhang, D. Li, Adsorptive removal of phosphate from water using mesoporous materials: a review, J. Environ. Manage., 193 (2017) 470–482.

[24] X.D. Zhang, Y. Wang, Y.Q. Yang, D. Chen, Recent progress in the removal of volatile organic compounds by mesoporous silica materials and supported catalysts, Wuli Huaxue Xuebao/Acta Phys. Chim. Sin., 31 (2015) 1633–1646.

[25] Z. Guo, J. Huang, Z. Xue, X. Wang, Electrospun graphene oxide/carbon composite nanofibers with well-developed mesoporous structure and their adsorption performance for benzene and butanone, Chem. Eng. J., 306 (2016) 99–106.

[26] S.M. Manocha, Porous carbons, Sadhana - Acad. Proc. Eng. Sci., 28 (2003) 335–348.

[27] D. Thatikayala, M.T. Noori, B. Min, Zeolite-modified electrodes for electrochemical sensing of heavy metal ions – progress and future directions, Mater. Today Chem., 29 (2023) 101412, doi: 10.1016/j.mtchem.2023.101412.

[28] G. Férey, Hybrid porous solids: past, present, future, Chem. Soc. Rev., 37 (2008) 191–214.

[29] M. Wen, Y. Kuwahara, K. Mori, D. Zhang, H. Li, H. Yamashita, Synthesis of Ce ions doped metal–organic framework for promoting catalytic H_2 production from ammonia borane under visible light irradiation, J. Mater. Chem. A, 3 (2015) 14134–14141.

[30] M. Wen, Y. Cui, Y. Kuwahara, K. Mori, H. Yamashita, Non-noble-metal nanoparticle supported on metal–organic framework as

an efficient and durable catalyst for promoting H_2 production from ammonia borane under visible light irradiation, ACS Appl. Mater. Interfaces, 8 (2016) 21278–21284.
[31] J.-L. Wang, C. Wang, W. Lin, Metal–organic frameworks for light harvesting and photocatalysis, ACS Catal., 2 (2012) 2630–2640.
[32] J. Seo, R. Matsuda, H. Sakamoto, C. Bonneau, S. Kitagawa, A pillared-layer coordination polymer with a rotatable pillar acting as a molecular gate for guest molecules, J. Am. Chem. Soc., 131 (2009) 12792–12800.
[33] T. Loiseau, C. Serre, C. Huguenard, G. Fink, F. Taulelle, M. Henry, T. Bataille, G. Férey, A rationale for the large breathing of the porous aluminum terephthalate (MIL-53) upon hydration, Chem. - A Eur. J., 10 (2004) 1373–1382.
[34] A. Schneemann, V. Bon, I. Schwedler, I. Senkovska, S. Kaskel, R.A. Fischer, Flexible metal–organic frameworks, Chem. Soc. Rev., 43 (2014) 6062–6096.
[35] Z.J. Lin, J. Lü, M. Hong, R. Cao, Metal–organic frameworks based on flexible ligands (FL-MOFs): structures and applications, Chem. Soc. Rev., 43 (2014) 5867–5895.
[36] O.K. Farha, I. Eryazici, N.C. Jeong, B.G. Hauser, C.E. Wilmer, A.A. Sarjeant, R.Q. Snurr, S.T. Nguyen, A.Ö. Yazaydın, J.T. Hupp, Metal–organic framework materials with ultrahigh surface areas: is the sky the limit?, J. Am. Chem. Soc., 134 (2012) 15016–15021.
[37] A. Demessence, D.M. D'Alessandro, M.L. Foo, J.R. Long, Strong CO_2 binding in a water-stable, triazolate-bridged metal–organic framework functionalized with ethylenediamine, J. Am. Chem. Soc., 131 (2009) 8784–8786.
[38] X.-Y. Lin, Y.-H. Li, M.-Y. Qi, Z.-R. Tang, H.-L. Jiang, Y.-J. Xu, A unique coordination-driven route for the precise nanoassembly of metal sulfides on metal–organic frameworks, Nanoscale Horiz., 5 (2020) 714–719.
[39] X.-Y. Lin, M.-Y. Qi, Z.-R. Tang, Y.-J. Xu, Photochemical dehydrogenation of N-heterocycles over MOF-supported CdS nanoparticles with nickel modification, Appl. Catal., B, 317 (2022) 121708, doi: 10.1016/j.apcatb.2022.121708.
[40] A.S. Malik, D. Letson, S.R. Crutchfield, Point/nonpoint source trading of pollution abatement: choosing the right trading ratio, Am. J. Agric. Econ., 75 (1993) 959–967.
[41] Y. Yang, B. Yan, W. Shen, Assessment of point and nonpoint sources pollution in Songhua River Basin, Northeast China by using revised water quality model, Chin. Geogr. Sci., 20 (2010) 30–36.
[42] S.R. Carpenter, N.F. Caraco, D.L. Correll, R.W. Howarth, A.N. Sharpley, V.H. Smith, Nonpoint pollution of surface waters with phosphorus and nitrogen, Ecol. Appl., 8 (1998) 559–568.
[43] N. Štambuk-Giljanović, The Pollution load by nitrogen and phosphorus IN the Jadro River, Environ. Monit. Assess., 123 (2006) 13–30.
[44] V. Kertész, G. Bakonyi, B. Farkas, Water pollution by Cu and Pb can adversely affect mallard embryonic development, Ecotoxicol. Environ. Saf., 65 (2006) 67–73.
[45] W. Ouyang, H. Huang, F. Hao, Y. Shan, B. Guo, Evaluating spatial interaction of soil property with non-point source pollution at watershed scale: the phosphorus indicator in Northeast China, Sci. Total Environ., 432 (2012) 412–421.
[46] J. Cheng, T. Yuan, W. Wang, J. Jia, X. Lin, L. Qu, Z. Ding, Mercury pollution in two typical areas in Guizhou Province, China and its neurotoxic effects in the brains of rats fed with local polluted rice, Environ. Geochem. Health, 28 (2006) 499–507.
[47] R. Lohmann, K. Breivik, J. Dachs, D. Muir, Global fate of POPs: current and future research directions, Environ. Pollut., 150 (2007) 150–165.
[48] K. Breivik, R. Alcock, Y.-F. Li, R.E. Bailey, H. Fiedler, J.M. Pacyna, Primary sources of selected POPs: regional and global scale emission inventories, Environ. Pollut., 128 (2004) 3–16.
[49] C.A. Basar, A. Karagunduz, A. Cakici, B. Keskinler, Removal of surfactants by powdered activated carbon and microfiltration, Water Res., 38 (2004) 2117–2124.
[50] K. Hunger, Industrial Dyes: Chemistry, Properties, Wiley, London, 2003.
[51] J. Michałowicz, W. Duda, Phenols - sources and toxicity, Pol. J. Environ. Stud., 16 (2007) 347–362.
[52] L. Theodore, Heat Transfer Applications for the Practicing Engineer, John Wiley & Sons, Ltd., Hoboken, NJ, USA, 2011.
[53] Y.-S. Ho, W.-T. Chiu, C.-C. Wang, Regression analysis for the sorption isotherms of basic dyes on sugarcane dust, Bioresour. Technol., 96 (2005) 1285–1291.
[54] H.M.F. Freundlich, Over the adsorption in solution, J. Phys. Chem., 57 (1906) 385–471.
[55] G. Tchobanoglous, F.L. Burton, H.D. Stensel, Wastewater Engineering: Treatment and Reuse, 4th ed., McGraw-Hill, Boston, 2003.
[56] C.A. Toles, W.E. Marshall, M.M. Johns, L.H. Wartelle, A. McAloon, Acid-activated carbons from almond shells: physical, chemical and adsorptive properties and estimated cost of production, Bioresour. Technol., 71 (2000) 87–92.
[57] C.A. Toles, W.E. Marshall, M.M. Johns, Phosphoric acid activation of nutshells for metals and organic remediation: process optimization, J. Chem. Technol. Biotechnol., 72 (1998) 255–263.
[58] M.M. Johns, W.E. Marshall, C.A. Toles, Agricultural by-products as granular activated carbons for adsorbing dissolved metals and organics, J. Chem. Technol. Biotechnol., 71 (1998) 131–140.
[59] S.A. Dastgheib, D.A. Rockstraw, Pecan shell activated carbon: synthesis, characterization, and application for the removal of copper from aqueous solution, Carbon N. Y., 39 (2001) 1849–1855.
[60] L.H. Wartelle, W.E. Marshall, Nutshells as granular activated carbons: physical, chemical and adsorptive properties, J. Chem. Technol. Biotechnol., 76 (2001) 451–455.
[61] T.S. Anirudhan, S.S. Sreekumari, Adsorptive removal of heavy metal ions from industrial effluents using activated carbon derived from waste coconut buttons, J. Environ. Sci., 23 (2011) 1989–1998.
[62] M. Ullah, R. Nazir, M. Khan, W. Khan, M. Shah, S.G. Afridi, A. Zada, The effective removal of heavy metals from water by activated carbon adsorbents of *Albizia lebbeck* and *Melia azedarach* seed shells, Soil Water Res., 15 (2020) 30–37.
[63] S. Iijima, Helical microtubules of graphitic carbon, Nature, 354 (1991) 56–58.
[64] D.S. Bethune, C.H. Kiang, M.S. de Vries, G. Gorman, R. Savoy, J. Vazquez, R. Beyers, Cobalt-catalysed growth of carbon nanotubes with single-atomic-layer walls, Nature, 363 (1993) 605–607.
[65] S.-H. Hsieh, J.-J. Horng, Adsorption behavior of heavy metal ions by carbon nanotubes grown on microsized Al_2O_3 particles, J. Univ. Sci. Technol. Beijing, Miner. Metall. Mater., 14 (2007) 77–84.
[66] A. Stafiej, K. Pyrzynska, Solid phase extraction of metal ions using carbon nanotubes, Microchem. J., 89 (2008) 29–33.
[67] G.P. Rao, C. Lu, F. Su, Sorption of divalent metal ions from aqueous solution by carbon nanotubes: a review, Sep. Purif. Technol., 58 (2007) 224–231.
[68] R.Q. Long, R.T. Yang, Carbon nanotubes as superior sorbent for dioxin removal, J. Am. Chem. Soc., 123 (2001) 2058–2059.
[69] X. Peng, Y. Li, Z. Luan, Z. Di, H. Wang, B. Tian, Z. Jia, Adsorption of 1,2-dichlorobenzene from water to carbon nanotubes, Chem. Phys. Lett., 376 (2003) 154–158.
[70] C. Lu, C. Liu, G.P. Rao, Comparisons of sorbent cost for the removal of Ni^{2+} from aqueous solution by carbon nanotubes and granular activated carbon, J. Hazard. Mater., 151 (2008) 239–246.
[71] F. Fornasiero, H.G. Park, J.K. Holt, M. Stadermann, C.P. Grigoropoulos, A. Noy, O. Bakajin, Ion exclusion by sub-2-nm carbon nanotube pores, Proc. Natl. Acad. Sci. U.S.A., 105 (2008) 17250–17255.
[72] N. Savage, M.S. Diallo, Nanomaterials and water purification: opportunities and challenges, J. Nanopart. Res., 7 (2005) 331–342.
[73] K.S. Novoselov, V.I. Fal'ko, L. Colombo, P.R. Gellert, M.G. Schwab, K. Kim, A roadmap for graphene, Nature, 490 (2012) 192–200.

[74] W. Gao, M. Majumder, L.B. Alemany, T.N. Narayanan, M.A. Ibarra, B.K. Pradhan, P.M. Ajayan, Engineered graphite oxide materials for application in water purification, ACS Appl. Mater. Interfaces, 3 (2011) 1821–1826.
[75] P. Avouris, C. Dimitrakopoulos, Graphene: synthesis and applications, Mater. Today, 15 (2012) 86–97.
[76] L. Xu, J. Wang, The application of graphene-based materials for the removal of heavy metals and radionuclides from water and wastewater, Crit. Rev. Env. Sci. Technol., 47 (2017) 1042–1105.
[77] Q. Qin, Q. Wang, D. Fu, J. Ma, An efficient approach for Pb(II) and Cd(II) removal using manganese dioxide formed in situ, Chem. Eng. J., 172 (2011) 68–74.
[78] G. Zhao, J. Li, X. Ren, C. Chen, X. Wang, Few-layered graphene oxide nanosheets as superior sorbents for heavy metal ion pollution management, Environ. Sci. Technol., 45 (2011) 10454–10462.
[79] F. Arshad, M. Selvaraj, J. Zain, F. Banat, M.A. Haija, Polyethylenimine modified graphene oxide hydrogel composite as an efficient adsorbent for heavy metal ions, Sep. Purif. Technol., 209 (2019) 870–880.
[80] D. Vilela, J. Parmar, Y. Zeng, Y. Zhao, S. Sánchez, Graphene-based microbots for toxic heavy metal removal and recovery from water, Nano Lett., 16 (2016) 2860–2866.
[81] M. Inada, Y. Eguchi, N. Enomoto, J. Hojo, Synthesis of zeolite from coal fly ashes with different silica–alumina composition, Fuel, 84 (2005) 299–304.
[82] X. Querol, N. Moreno, J.C. Umaa, R. Juan, S. Hernndez, C. Fernandez-Pereira, C. Ayora, M. Janssen, J. Garca-Martnez, A. Linares-Solano, D. Cazorla-Amoros, Application of zeolitic material synthesised from fly ash to the decontamination of waste water and flue gas, J. Chem. Technol. Biotechnol., 77 (2002) 292–298.
[83] L. Bandura, M. Franus, G. Józefaciuk, W. Franus, Synthetic zeolites from fly ash as effective mineral sorbents for land-based petroleum spills cleanup, Fuel, 147 (2015) 100–107.
[84] B. Szala, T. Bajda, J. Matusik, K. Zięba, B. Kijak, BTX sorption on Na-P1 organo-zeolite as a process controlled by the amount of adsorbed HDTMA, Microporous Mesoporous Mater., 202 (2015) 115–123.
[85] I.G. Stefanova, Natural Sorbents as Barriers Against Migration of Radionuclides from Radioactive Waste Repositories BT, P. Misaelides, F. Macášek, T.J. Pinnavaia, C. Colella, Eds., Natural Microporous Materials in Environmental Technology, Springer, Netherlands, Dordrecht, 1999, pp. 371–379.
[86] L. Sörme, A. Lindqvist, H. Söderberg, Capacity to influence sources of heavy metals to wastewater treatment sludge, Environ. Manage., 31 (2003) 421–428.
[87] T. Lee, L. Deog-Bae, L. Kyeong-Bo, H. Sang-Bok, H. Sang-Soo, Sorption of heavy metals from the wastewater by the artificial zeolite, Korean J. Soil Sci. Fert., 31 (1998) 61–66.
[88] C. Haidouti, Inactivation of mercury in contaminated soils using natural zeolites, Sci. Total Environ., 208 (1997) 105–109.
[89] J. Morency, Zeolite sorbent that effectively removes mercury from flue gases, Filtr. Sep., 39 (2002) 24–26.
[90] M. Wdowin, M.M. Wiatros-Motyka, R. Panek, L.A. Stevens, W. Franus, C.E. Snape, Experimental study of mercury removal from exhaust gases, Fuel, 128 (2014) 451–457.
[91] M.W. Ackley, S.U. Rege, H. Saxena, Application of natural zeolites in the purification and separation of gases, Microporous Mesoporous Mater., 61 (2003) 25–42.
[92] G. Zhao, X. Huang, Z. Tang, Q. Huang, F. Niu, X. Wang, Polymer-based nanocomposites for heavy metal ions removal from aqueous solution: a review, Polym. Chem., 9 (2018) 3562–3582.
[93] F. Lu, D. Astruc, Nanomaterials for removal of toxic elements from water, Coord. Chem. Rev., 356 (2018) 147–164.
[94] Y. Zhang, B. Wu, H. Xu, H. Liu, M. Wang, Y. He, B. Pan, Nanomaterials-enabled water and wastewater treatment, NanoImpact, 3–4 (2016) 22–39.
[95] G.N. Manju, K. Anoop Krishnan, V.P. Vinod, T.S. Anirudhan, An investigation into the sorption of heavy metals from wastewaters by polyacrylamide-grafted iron(III) oxide, J. Hazard. Mater., 91 (2002) 221–238.
[96] A. Afshar, S.A.S. Sadjadi, A. Mollahosseini, M.R. Eskandarian, Polypyrrole-polyaniline/Fe_3O_4 magnetic nanocomposite for the removal of Pb(II) from aqueous solution, Korean J. Chem. Eng., 33 (2016) 669–677.
[97] J. Cai, M. Lei, Q. Zhang, J.-R. He, T. Chen, S. Liu, S.-H. Fu, T.-T. Li, G. Liu, P. Fei, Electrospun composite nanofiber mats of cellulose@organically modified montmorillonite for heavy metal ion removal: design, characterization, evaluation of absorption performance, Composites, Part A, 92 (2017) 10–16.
[98] Suman, A. Kardam, M. Gera, V.K. Jain, A novel reusable nanocomposite for complete removal of dyes, heavy metals and microbial load from water based on nanocellulose and silver nano-embedded pebbles, Environ. Technol., 36 (2015) 706–714.
[99] A.H.A. Saad, A.M. Azzam, S.T. El-Wakeel, B.B. Mostafa, M.B. Abd El-latif, Removal of toxic metal ions from wastewater using ZnO@chitosan core-shell nanocomposite, Environ. Nanotechnol. Monit. Manage., 9 (2018) 67–75.
[100] S. Gokila, T. Gomathi, P.N. Sudha, S. Anil, Removal of the heavy metal ion chromiuim(VI) using chitosan and alginate nanocomposites, Int. J. Biol. Macromol., 104 (2017) 1459–1468.
[101] G. Lofrano, M. Carotenuto, G. Libralato, R.F. Domingos, A. Markus, L. Dini, R.K. Gautam, D. Baldantoni, M. Rossi, S.K. Sharma, M.C. Chattopadhyaya, M. Giugni, S. Meric, Polymer functionalized nanocomposites for metals removal from water and wastewater: an overview, Water Res., 92 (2016) 22–37.
[102] H.C.J. Zhou, S. Kitagawa, Metal–organic frameworks (MOFs), Chem. Soc. Rev., 43 (2014) 5415–5418.
[103] P. Kumar, V. Bansal, K.-H. Kim, E.E. Kwon, Metal–organic frameworks (MOFs) as futuristic options for wastewater treatment, J. Ind. Eng. Chem., 62 (2018) 130–145.
[104] L.P. Wang, G.Y. Wang, F. Wang, P.H. Wang, Effect of different aromatic carboxylic acid ligands on the catalytic activities of metal–organic frameworks, Adv. Mater. Res., 634–638 (2013) 513–517.
[105] K. Kowalski, Ferrocenyl-nucleobase complexes: Synthesis, chemistry and applications, Coord. Chem. Rev., 317 (2016) 132–156.
[106] Y. Bian, N. Xiong, G. Zhu, Technology for the remediation of water pollution: a review on the fabrication of metal–organic frameworks, Processes, 6 (2018) 1–22.
[107] W. Liu, H. Chen, 1D energetic metal–organic frameworks: synthesis and properties, Cailiao Daobao/Mater. Rev., 32 (2018) 223–227.
[108] J. Dai, X. Xiao, S. Duan, J. Liu, J. He, J. Lei, L. Wang, Synthesis of novel microporous nanocomposites of ZIF-8 on multiwalled carbon nanotubes for adsorptive removing benzoic acid from water, Chem. Eng. J., 331 (2018) 64–74.
[109] H. Guo, Z. Zheng, Y. Zhang, H. Lin, Q. Xu, Highly selective detection of Pb^{2+} by a nanoscale Ni-based metal–organic framework fabricated through one-pot hydrothermal reaction, Sens. Actuators, B, 248 (2017) 430–436.
[110] S. Kitagawa, M. Kondo, Functional micropore chemistry of crystalline metal complex-assembled compounds, Bull. Chem. Soc. Jpn., 71 (1998) 1739–1753.
[111] Z. Wang, S.M. Cohen, Postsynthetic modification of metal–organic frameworks, Chem. Soc. Rev., 38 (2009) 1315–1329.
[112] S.M. Cohen, Postsynthetic methods for the functionalization of metal–organic frameworks, Chem. Rev., 112 (2012) 970–1000.
[113] J. Liu, L. Chen, H. Cui, J. Zhang, L. Zhang, C.Y. Su, Applications of metal–organic frameworks in heterogeneous supramolecular catalysis, Chem. Soc. Rev., 43 (2014) 6011–6061.
[114] B. Li, H.-M. Wen, W. Zhou, B. Chen, Porous Metal–organic frameworks for gas storage and separation: what, how, and why?, J. Phys. Chem. Lett., 5 (2014) 3468–3479.
[115] B. Li, H. Wang, B. Chen, Microporous metal–organic frameworks for gas separation, Chem. - An Asian J., 9 (2014) 1474–1498.
[116] Y. Huang, S.C. Lee, K.F. Ho, S.S.H. Ho, N. Cao, Y. Cheng, Y. Gao, Effect of ammonia on ozone-initiated formation of

indoor secondary products with emissions from cleaning products, Atmos. Environ., 59 (2012) 224–231.
[117] B.O. Bolaji, Z. Huan, Ozone depletion and global warming: case for the use of natural refrigerant – a review, Renewable Sustainable Energy Rev., 18 (2013) 49–54.
[118] G.W. Peterson, G.W. Wagner, A. Balboa, J. Mahle, T. Sewell, C.J. Karwacki, Ammonia vapor removal by $Cu_3(BTC)_2$ and its characterization by MAS NMR, J. Phys. Chem. C, 113 (2009) 13906–13917.
[119] P.A. Kobielska, A.J. Howarth, O.K. Farha, S. Nayak, Metal–organic frameworks for heavy metal removal from water, Coord. Chem. Rev., 358 (2018) 92–107.
[120] M.J. Katz, A.J. Howarth, P.Z. Moghadam, J.B. DeCoste, R.Q. Snurr, J.T. Hupp, O.K. Farha, High volumetric uptake of ammonia using Cu-MOF-74/Cu-CPO-27, Dalton Trans., 45 (2016) 4150–4153.
[121] A.J. Rieth, Y. Tulchinsky, M. Dincă, High and reversible ammonia uptake in mesoporous azolate metal–organic frameworks with open Mn, Co, and Ni sites, J. Am. Chem. Soc., 138 (2016) 9401–9404.
[122] K.C. Kim, P.Z. Moghadam, D. Fairen-Jimenez, R.Q. Snurr, Computational screening of metal catecholates for ammonia capture in metal–organic frameworks, Ind. Eng. Chem. Res., 54 (2015) 3257–3267.
[123] J.N. Joshi, E.Y. Garcia-Gutierrez, C.M. Moran, J.I. Deneff, K.S. Walton, Engineering copper carboxylate functionalities on water stable metal–organic frameworks for enhancement of ammonia removal capacities, J. Phys. Chem. C, 121 (2017) 3310–3319.
[124] N.M. Padial, E. Quartapelle-Procopio, C. Montoro, E. López, J.E. Oltra, V. Colombo, A. Maspero, N. Masciocchi, S. Galli, I. Senkovska, S. Kaskel, E. Barea, J.A.R. Navarro, Highly hydrophobic isoreticular porous metal–organic frameworks for the capture of harmful volatile organic compounds, Angew. Chem. Int. Ed., 52 (2013) 8290–8294.
[125] Z. Zhao, S. Wang, Y. Yang, X. Li, J. Li, Z. Li, Competitive adsorption and selectivity of benzene and water vapor on the microporous metal–organic frameworks (HKUST-1), Chem. Eng. J., 259 (2015) 79–89.
[126] A. Planchais, S. Devautour-Vinot, S. Giret, F. Salles, P. Trens, A. Fateeva, T. Devic, P. Yot, C. Serre, N. Ramsahye, G. Maurin, Adsorption of benzene in the cation-containing MOFs MIL-141, J. Phys. Chem. C, 117 (2013) 19393–19401.
[127] W.W. He, G.S. Yang, Y.J. Tang, S.L. Li, S.R. Zhang, Z.M. Su, Y.Q. Lan, Phenyl groups result in the highest benzene storage and most efficient desulfurization in a series of isostructural metal–organic frameworks, Chem. - A Eur. J., 21 (2015) 9784–9789.
[128] D. Ma, Y. Li, Z. Li, Tuning the moisture stability of metal–organic frameworks by incorporating hydrophobic functional groups at different positions of ligands, Chem. Commun., 47 (2011) 7377–7379.
[129] W. Huang, J. Jiang, D. Wu, J. Xu, B. Xue, A.M. Kirillov, A highly stable nanotubular MOF rotator for selective adsorption of benzene and separation of xylene isomers, Inorg. Chem., 54 (2015) 10524–10526.
[130] G.W. Peterson, J.J. Mahle, J.B. DeCoste, W.O. Gordon, J.A. Rossin, Extraordinary NO_2 removal by the metal–organic framework UiO-66-NH_2, Angew. Chem., 128 (2016) 6343–6346.
[131] A.M. Ebrahim, T.J. Bandosz, Effect of amine modification on the properties of zirconium–carboxylic acid based materials and their applications as NO_2 adsorbents at ambient conditions, Microporous Mesoporous Mater., 188 (2014) 149–162.
[132] C.O. Audu, H.G.T. Nguyen, C.Y. Chang, M.J. Katz, L. Mao, O.K. Farha, J.T. Hupp, S.T. Nguyen, The dual capture of As^V and As^{III} by UiO-66 and analogues, Chem. Sci., 7 (2016) 6492–6498.
[133] J.B. DeCoste, T.J. Demasky, M.J. Katz, O.K. Farha, J.T. Hupp, A UiO-66 analogue with uncoordinated carboxylic acids for the broad-spectrum removal of toxic chemicals, New J. Chem., 39 (2015) 2396–2399.
[134] J.Y. Lee, T.C. Keener, Y.J. Yang, Potential flue gas impurities in carbon dioxide streams separated from coal-fired power plants, J. Air Waste Manage. Assoc., 59 (2009) 725–732.
[135] K. Tan, P. Canepa, Q. Gong, J. Liu, D.H. Johnson, A. Dyevoich, P.K. Thallapally, T. Thonhauser, J. Li, Y.J. Chabal, Mechanism of preferential adsorption of SO_2 into two microporous paddle wheel frameworks $M(bdc)(ted)_{0.5}$, Chem. Mater., 25 (2013) 4653–4662.
[136] M. Savage, Y. Cheng, T.L. Easun, J.E. Eyley, S.P. Argent, M.R. Warren, W. Lewis, C. Murray, C.C. Tang, M.D. Frogley, G. Cinque, J. Sun, S. Rudić, R.T. Murden, M.J. Benham, A.N. Fitch, A.J. Blake, A.J. Ramirez-Cuesta, S. Yang, M. Schröder, Selective adsorption of sulfur dioxide in a robust metal–organic framework material, Adv. Mater., 28 (2016) 8705–8711.
[137] X. Cui, Q. Yang, L. Yang, R. Krishna, Z. Zhang, Z. Bao, H. Wu, Q. Ren, W. Zhou, B. Chen, H. Xing, Ultrahigh and selective SO_2 uptake in inorganic anion-pillared hybrid porous materials, Adv. Mater., 29 (2017) 1606929, doi: 10.1002/adma.201606929.
[138] C.E. Uzoigwe, L.C.S. Franco, M.D. Forrest, Iatrogenic Greenhouse Gases: The Role of Anaesthetic Agents, British Journal Hospital Medicine, MA Healthcare London, 2016, pp. 19–23.
[139] Y. Ishizawa, General anesthetic gases and the global environment, Anesth. Analg., 112 (2011) 213–217.
[140] N. Gargiulo, A. Peluso, P. Aprea, M. Eić, D. Caputo, An insight into clustering of halogenated anesthetics molecules in metal–organic frameworks: evidence of adsorbate self-association in micropores, J. Colloid Interface Sci., 554 (2019) 463–467.
[141] N. Gargiulo, A. Peluso, P. Aprea, Y. Hua, D. Filipović, D. Caputo, M. Eić, A chromium-based metal–organic framework as a potential high performance adsorbent for anaesthetic vapours, RSC Adv., 4 (2014) 49478–49484.
[142] R.C. Ewing, F.N. von Hippel, Nuclear waste management in the United States—starting over, Science, 325 (2009) 151–152.
[143] K.W. Chapman, P.J. Chupas, T.M. Nenoff, Radioactive iodine capture in silver-containing mordenites through nanoscale silver iodide formation, J. Am. Chem. Soc., 132 (2010) 8897–8899.
[144] J.-P. Lang, Q.-F. Xu, R.-X. Yuan, B.F. Abrahams, [WS_4Cu_4(4,4′-bpy)4][$WS_4Cu_4I_4$(4,4′-bpy)2]]infinity--an unusual 3D porous coordination polymer formed from the preformed cluster $[Et_4N]_4[WS_4Cu_4I_6]$, Angew. Chem. Int. Ed., 43 (2004) 4741–4745.
[145] Z.-M. Wang, Y.-J. Zhang, T. Liu, M. Kurmoo, S. Gao, $[Fe_3(HCOO)_6]$: a permanent porous diamond framework displaying H_2/N_2 adsorption, guest inclusion, and guest-dependent magnetism, Adv. Funct. Mater., 17 (2007) 1523–1536.
[146] M.-H. Zeng, Q.-X. Wang, Y.-X. Tan, S. Hu, H.-X. Zhao, L.-S. Long, M. Kurmoo, Rigid pillars and double walls in a porous metal–organic framework: single-crystal to single-crystal, controlled uptake and release of iodine and electrical conductivity, J. Am. Chem. Soc., 132 (2010) 2561–2563.
[147] D.F. Sava, M.A. Rodriguez, K.W. Chapman, P.J. Chupas, J.A. Greathouse, P.S. Crozier, T.M. Nenoff, Capture of volatile iodine, a gaseous fission product, by zeolitic imidazolate framework-8, J. Am. Chem. Soc., 133 (2011) 12398–12401.
[148] D. Haefner, T. Tranter, Methods of Gas Phase Capture of Iodine From Fuel Reprocessing Off-Gas: A Literature Survey, Idaho National Laboratory, Idaho Falls, Idaho 83415, 2007, pp. 1–25.
[149] T.D. Bennett, P.J. Saines, D.A. Keen, J.-C. Tan, A.K. Cheetham, Ball-milling-induced amorphization of zeolitic imidazolate frameworks (ZIFs) for the irreversible trapping of iodine, Chem. - A Eur. J., 19 (2013) 7049–7055.
[150] F.G. Kerry, Industrial Gas Handbook: Gas Separation and Purification, CRC Press, Boca Raton, 2007.
[151] M.A. Torcivia, S.M.E. Demers, K.L. Broadwater, D.B. Hunter, Investigating the effects of Ag, Cu, and Pd functionalized chabazite on the adsorption affinities of noble gases Xe, Kr, and Ar, J. Phys. Chem. C, 127 (2023) 3800–3807.
[152] U. Mueller, M. Schubert, F. Teich, H. Puetter, K. Schierle-Arndt, J. Pastré, Metal–organic frameworks—prospective industrial applications, J. Mater. Chem., 16 (2006) 626–636.

[153] P.K. Thallapally, J.W. Grate, R.K. Motkuri, Facile xenon capture and release at room temperature using a metal–organic framework: a comparison with activated charcoal, Chem. Commun., 48 (2012) 347–349.
[154] J. Liu, P.K. Thallapally, D. Strachan, Metal–organic frameworks for removal of Xe and Kr from nuclear fuel reprocessing plants, Langmuir, 28 (2012) 11584–11589.
[155] D. Britt, D. Tranchemontagne, O.M. Yaghi, metal–organic frameworks with high capacity and selectivity for harmful gases, Proc. Natl. Acad. Sci. U.S.A., 105 (2008) 11623–11627.
[156] C.-Y. Huang, M. Song, Z.-Y. Gu, H.-F. Wang, X.-P. Yan, Probing the adsorption characteristic of metal–organic framework MIL-101 for volatile organic compounds by quartz crystal microbalance, Environ. Sci. Technol., 45 (2011) 4490–4496.
[157] K. Yang, Q. Sun, F. Xue, D. Lin, Adsorption of volatile organic compounds by metal–organic frameworks MIL-101: influence of molecular size and shape, J. Hazard. Mater., 195 (2011) 124–131.
[158] Z. Zhao, X. Li, S. Huang, Q. Xia, Z. Li, Adsorption and diffusion of benzene on chromium-based metal–organic framework MIL-101 synthesized by microwave irradiation, Ind. Eng. Chem. Res., 50 (2011) 2254–2261.
[159] E. Quartapelle Procopio, F. Linares, C. Montoro, V. Colombo, A. Maspero, E. Barea, J.A.R. Navarro, Cation-exchange porosity tuning in anionic metal–organic frameworks for the selective separation of gases and vapors and for catalysis, Angew. Chem., 122 (2010) 7466–7469.
[160] V. Finsy, C.E.A. Kirschhock, G. Vedts, M. Maes, L. Alaerts, D.E. De Vos, G.V. Baron, J.F.M. Denayer, Framework breathing in the vapour-phase adsorption and separation of xylene isomers with the metal–organic framework MIL-53, Chem. - A Eur. J., 15 (2009) 7724–7731.
[161] H. Wu, Q. Gong, D.H. Olson, J. Li, Commensurate adsorption of hydrocarbons and alcohols in microporous metal–organic frameworks, Chem. Rev., 112 (2012) 836–868.
[162] N.A. Khan, S.H. Jhung, Remarkable adsorption capacity of $CuCl_2$-loaded porous vanadium benzenedicarboxylate for benzothiophene, Angew. Chem. Int. Ed., 51 (2012) 1198–1201.
[163] Y. Takashima, V.M. Martínez, S. Furukawa, M. Kondo, S. Shimomura, H. Uehara, M. Nakahama, K. Sugimoto, S. Kitagawa, Molecular decoding using luminescence from an entangled porous framework, Nat. Commun., 2 (2011) 168, doi: 10.1038/ncomms1170.
[164] M. Ohba, K. Yoneda, G. Agustí, M.C. Muñoz, A.B. Gaspar, J.A. Real, M. Yamasaki, H. Ando, Y. Nakao, S. Sakaki, S. Kitagawa, Bidirectional chemo-switching of spin state in a microporous framework, Angew. Chem. Int. Ed., 48 (2009) 4767–4771.
[165] S. Galli, N. Masciocchi, V. Colombo, A. Maspero, G. Palmisano, F.J. López-Garzón, M. Domingo-García, I. Fernández-Morales, E. Barea, J.A.R. Navarro, Adsorption of harmful organic vapors by flexible hydrophobic bis-pyrazolate based MOFs, Chem. Mater., 22 (2010) 1664–1672.
[166] C. Montoro, F. Linares, E. Quartapelle Procopio, I. Senkovska, S. Kaskel, S. Galli, N. Masciocchi, E. Barea, J.A.R. Navarro, Capture of nerve agents and mustard gas analogues by hydrophobic robust MOF-5 type metal–organic frameworks, J. Am. Chem. Soc., 133 (2011) 11888–11891.
[167] C. Yang, U. Kaipa, Q.Z. Mather, X. Wang, V. Nesterov, A.F. Venero, M.A. Omary, Fluorous metal–organic frameworks with superior adsorption and hydrophobic properties toward oil spill cleanup and hydrocarbon storage, J. Am. Chem. Soc., 133 (2011) 18094–18097.
[168] A. Pell, A. Márquez, J.F. López-Sánchez, R. Rubio, M. Barbero, S. Stegen, F. Queirolo, P. Díaz-Palma, Occurrence of arsenic species in algae and freshwater plants of an extreme arid region in northern Chile, the Loa River Basin, Chemosphere, 90 (2013) 556–564.
[169] R.E. Vernon, Which elements are metalloids?, J. Chem. Educ., 90 (2013) 1703–1707.
[170] B.-J. Zhu, X.-Y. Yu, Y. Jia, F.-M. Peng, B. Sun, M.-Y. Zhang, T. Luo, J.-H. Liu, X.-J. Huang, Iron and 1,3,5-benzenetricarboxylic metal–organic coordination polymers prepared by solvothermal method and their application in efficient As(V) removal from aqueous solutions, J. Phys. Chem. C, 116 (2012) 8601–8607.
[171] Z.-Q. Li, J.-C. Yang, K.-W. Sui, N. Yin, Facile synthesis of metal–organic framework MOF-808 for arsenic removal, Mater. Lett., 160 (2015) 412–414.
[172] C. Prum, R. Dolphen, P. Thiravetyan, Enhancing arsenic removal from arsenic-contaminated water by *Echinodorus cordifolius*–endophytic *Arthrobacter creatinolyticus* interactions, J. Environ. Manage., 213 (2018) 11–19.
[173] T.A. Vu, G.H. Le, C.D. Dao, L.Q. Dang, K.T. Nguyen, Q.K. Nguyen, P.T. Dang, H.T.K. Tran, Q.T. Duong, T.V. Nguyen, G.D. Lee, Arsenic removal from aqueous solutions by adsorption using novel MIL-53(Fe) as a highly efficient adsorbent, RSC Adv., 5 (2015) 5261–5268.
[174] M. Filella, N. Belzile, Y.-W. Chen, Antimony in the environment: a review focused on natural waters: I. Occurrence, Earth-Sci. Rev., 57 (2002) 125–176.
[175] T.E. McKone, J.I. Daniels, Estimating human exposure through multiple pathways from air, water, and soil, Regul. Toxicol. Pharm., 13 (1991) 36–61.
[176] J.E. Mondloch, W. Bury, D. Fairen-Jimenez, S. Kwon, E.J. DeMarco, M.H. Weston, A.A. Sarjeant, S.T. Nguyen, P.C. Stair, R.Q. Snurr, O.K. Farha, J.T. Hupp, Vapor-phase metalation by atomic layer deposition in a metal–organic framework, J. Am. Chem. Soc., 135 (2013) 10294–10297.
[177] A.J. Howarth, Y. Liu, P. Li, Z. Li, T.C. Wang, J.T. Hupp, O.K. Farha, Chemical, thermal and mechanical stabilities of metal–organic frameworks, Nat. Rev. Mater., 1 (2016) 15018, doi: 10.1038/natrevmats.2015.18.
[178] A.J. Howarth, M.J. Katz, T.C. Wang, A.E. Platero-Prats, K.W. Chapman, J.T. Hupp, O.K. Farha, High efficiency adsorption and removal of selenate and selenite from water using metal–organic frameworks, J. Am. Chem. Soc., 137 (2015) 7488–7494.
[179] S. Rangwani, A.J. Howarth, M.R. DeStefano, C.D. Malliakas, A.E. Platero-Prats, K.W. Chapman, O.K. Farha, Adsorptive removal of Sb(V) from water using a mesoporous Zr-based metal–organic framework, Polyhedron, 151 (2018) 338–343.
[180] J. Li, X. Li, T. Hayat, A. Alsaedi, C. Chen, Screening of zirconium-based metal–organic frameworks for efficient simultaneous removal of antimonite (Sb(III)) and antimonate (Sb(V)) from aqueous solution, ACS Sustainable Chem. Eng., 5 (2017) 11496–11503.
[181] M. Kim, S.M. Cohen, Discovery, development, and functionalization of Zr(IV)-based metal–organic frameworks, CrystEngComm, 14 (2012) 4096–4104.
[182] X. He, X. Min, X. Luo, Efficient removal of antimony (III, V) from contaminated water by amino modification of a zirconium metal–organic framework with mechanism study, J. Chem. Eng. Data, 62 (2017) 1519–1529.
[183] F. Ke, L.-G. Qiu, Y.-P. Yuan, F.-M. Peng, X. Jiang, A.-J. Xie, Y.-H. Shen, J.-F. Zhu, Thiol-functionalization of metal–organic framework by a facile coordination-based postsynthetic strategy and enhanced removal of Hg^{2+} from water, J. Hazard. Mater., 196 (2011) 36–43.
[184] L. Huang, M. He, B. Chen, B. Hu, A designable magnetic MOF composite and facile coordination-based post-synthetic strategy for the enhanced removal of Hg^{2+} from water, J. Mater. Chem. A, 3 (2015) 11587–11595.
[185] H. Saleem, U. Rafique, R.P. Davies, Investigations on post-synthetically modified UiO-66-NH_2 for the adsorptive removal of heavy metal ions from aqueous solution, Microporous Mesoporous Mater., 221 (2016) 238–244.
[186] K.-K. Yee, N. Reimer, J. Liu, S.-Y. Cheng, S.-M. Yiu, J. Weber, N. Stock, Z. Xu, Effective mercury sorption by thiol-laced metal–organic frameworks: in strong acid and the vapor phase, J. Am. Chem. Soc., 135 (2013) 7795–7798.
[187] S. Halder, J. Mondal, J. Ortega-Castro, A. Frontera, P. Roy, A Ni-based MOF for selective detection and removal of Hg^{2+} in aqueous medium: a facile strategy, Dalton Trans., 46 (2017) 1943–1950.

[188] Y. Manawi, G. McKay, N. Ismail, A. Kayvani Fard, V. Kochkodan, M.A. Atieh, Enhancing lead removal from water by complex-assisted filtration with acacia gum, Chem. Eng. J., 352 (2018) 828–836.
[189] R. Ricco, K. Konstas, M.J. Styles, J.J. Richardson, R. Babarao, K. Suzuki, P. Scopece, P. Falcaro, Lead(II) uptake by aluminium based magnetic framework composites (MFCs) in water, J. Mater. Chem. A, 3 (2015) 19822–19831.
[190] J. Zhang, Z. Xiong, C. Li, C. Wu, Exploring a thiol-functionalized MOF for elimination of lead and cadmium from aqueous solution, J. Mol. Liq., 221 (2016) 43–50.
[191] J.M. Rivera, S. Rincón, C. Ben Youssef, A. Zepeda, Highly efficient adsorption of aqueous Pb(II) with mesoporous metal–organic framework-5: an equilibrium and kinetic study, J. Nanomater., 2016 (2016) 8095737, doi: 10.1155/2016/8095737.
[192] E. Tahmasebi, M.Y. Masoomi, Y. Yamini, A. Morsali, Application of mechanosynthesized azine-decorated zinc(II) metal–organic frameworks for highly efficient removal and extraction of some heavy-metal ions from aqueous samples: a comparative study, Inorg. Chem., 54 (2015) 425–433.
[193] F. Zou, R. Yu, R. Li, W. Li, Microwave-assisted synthesis of HKUST-1 and functionalized HKUST-1-@$H_3PW_{12}O_{40}$: selective adsorption of heavy metal ions in water analyzed with synchrotron radiation, ChemPhysChem, 14 (2013) 2825–2832.
[194] E. Rahimi, N. Mohaghegh, Removal of toxic metal ions from sungun acid rock drainage using mordenite zeolite, graphene nanosheets, and a novel metal–organic framework, Mine Water Environ., 35 (2016) 18–28.
[195] Q. Yang, Q. Zhao, S. Ren, Q. Lu, X. Guo, Z. Chen, Fabrication of core-shell Fe_3O_4@MIL-100(Fe) magnetic microspheres for the removal of Cr(VI) in aqueous solution, J. Solid State Chem., 244 (2016) 25–30.
[196] L. Aboutorabi, A. Morsali, E. Tahmasebi, O. Büyükgüngor, Metal–organic framework based on isonicotinate N-oxide for fast and highly efficient aqueous phase Cr(VI) adsorption, Inorg. Chem., 55 (2016) 5507–5513.
[197] K. Wang, X. Tao, J. Xu, N. Yin, Novel chitosan–MOF composite adsorbent for the removal of heavy metal ions, Chem. Lett., 45 (2016) 1365–1368.
[198] S. Rapti, A. Pournara, D. Sarma, I.T. Papadas, G.S. Armatas, Y.S. Hassan, M.H. Alkordi, M.G. Kanatzidis, M.J. Manos, Rapid, green and inexpensive synthesis of high quality UiO-66 amino-functionalized materials with exceptional capability for removal of hexavalent chromium from industrial waste, Inorg. Chem. Front., 3 (2016) 635–644.
[199] A. Ma, F. Ke, J. Jiang, Q. Yuan, Z. Luo, J. Liu, A. Kumar, Two lanthanide-based metal–organic frameworks for highly efficient adsorption and removal of fluoride ions from water, CrystEngComm, 19 (2017) 2172–2177.
[200] M. Vithanage, P. Bhattacharya, Fluoride in the environment: sources, distribution and defluoridation, Environ. Chem. Lett., 13 (2015) 131–147.
[201] N. Zhang, X. Yang, X. Yu, Y. Jia, J. Wang, L. Kong, Z. Jin, B. Sun, T. Luo, J. Liu, Al-1,3,5-benzenetricarboxylic metal–organic frameworks: a promising adsorbent for defluoridation of water with pH insensitivity and low aluminum residual, Chem. Eng. J., 252 (2014) 220–229.
[202] K.-Y.A. Lin, Y.-T. Liu, S.-Y. Chen, Adsorption of fluoride to UiO-66-NH_2 in water: stability, kinetic, isotherm and thermodynamic studies, J. Colloid Interface Sci., 461 (2016) 79–87.
[203] F. Ke, C. Peng, T. Zhang, M. Zhang, C. Zhou, H. Cai, J. Zhu, X. Wan, Fumarate-based metal–organic frameworks as a new platform for highly selective removal of fluoride from brick tea, Sci. Rep., 8 (2018) 939, doi: 10.1038/s41598-018-19277-2.
[204] X.-H. Zhu, C.-X. Yang, X.-P. Yan, Metal–organic framework-801 for efficient removal of fluoride from water, Microporous Mesoporous Mater., 259 (2018) 163–170.
[205] X. Zhang, F. Sun, J. He, H. Xu, F. Cui, W. Wang, Robust phosphate capture over inorganic adsorbents derived from lanthanum metal–organic frameworks, Chem. Eng. J., 326 (2017) 1086–1094.
[206] S. Mazloomi, M. Yousefi, H. Nourmoradi, M. Shams, Evaluation of phosphate removal from aqueous solution using metal–organic framework; isotherm, kinetic and thermodynamic study, J. Environ. Health Sci. Eng., 17 (2019) 209–218.
[207] H. Qiu, L. Yang, F. Liu, Y. Zhao, L. Liu, J. Zhu, M. Song, Highly selective capture of phosphate ions from water by a water stable metal–organic framework modified with polyethyleneimine, Environ. Sci. Pollut. Res., 24 (2017) 23694–23703.
[208] T. Liu, J. Feng, Y. Wan, S. Zheng, L. Yang, ZrO_2 nanoparticles confined in metal–organic frameworks for highly effective adsorption of phosphate, Chemosphere, 210 (2018) 907–916.
[209] K.-Y.A. Lin, S.-Y. Chen, A.P. Jochems, Zirconium-based metal–organic frameworks: highly selective adsorbents for removal of phosphate from water and urine, Mater. Chem. Phys., 160 (2015) 168–176.
[210] Y. Feng, H. Jiang, S. Li, J. Wang, X. Jing, Y. Wang, M. Chen, Metal–organic frameworks HKUST-1 for liquid-phase adsorption of uranium, Colloids Surf., A, 431 (2013) 87–92.
[211] D. Sheng, L. Zhu, C. Xu, C. Xiao, Y. Wang, Y. Wang, L. Chen, J. Diwu, J. Chen, Z. Chai, T.E. Albrecht-Schmitt, S. Wang, Efficient and selective uptake of TcO_4^- by a cationic metal–organic framework material with open Ag^+ sites, Environ. Sci. Technol., 51 (2017) 3471–3479.
[212] N. Zhang, L.-Y. Yuan, W.-L. Guo, S.-Z. Luo, Z.-F. Chai, W.-Q. Shi, Extending the use of highly porous and functionalized MOFs to Th(IV) capture, ACS Appl. Mater. Interfaces, 9 (2017) 25216–25224.
[213] R. Das, C.M. Nagaraja, Noble metal-free Cu(I)-anchored NHC-based MOF for highly recyclable fixation of CO_2 under RT and atmospheric pressure conditions, Green Chem., 23 (2021) 5195–5204.
[214] M. Wen, G. Li, H. Liu, J. Chen, T. An, H. Yamashita, Metal–organic framework-based nanomaterials for adsorption and photocatalytic degradation of gaseous pollutants: recent progress and challenges, Environ. Sci. Nano, 6 (2019) 1006–1025.
[215] M. Ding, X. Cai, H.-L. Jiang, Improving MOF stability: approaches and applications, Chem. Sci., 10 (2019) 10209–10230.
[216] P. Horcajada, C. Serre, G. Maurin, N.A. Ramsahye, F. Balas, M. Vallet-Regí, M. Sebban, F. Taulelle, G. Férey, Porous metal–organic-framework nanoscale carriers as a potential platform for drug delivery and imaging, J. Am. Chem. Soc., 130 (2008) 6774–6780.
[217] H.-L. Zhu, J.-R. Huang, P.-Q. Liao, X.-M. Chen, Rational design of metal–organic frameworks for electroreduction of CO_2 to hydrocarbons and carbon oxygenates, ACS Cent. Sci., 8 (2022) 1506–1517.
[218] C. Li, Z. Zhuang, F. Huang, Z. Wu, Y. Hong, Z. Lin, Recycling rare earth elements from industrial wastewater with flowerlike nano-$Mg(OH)_2$, ACS Appl. Mater. Interfaces, 5 (2013) 9719–9725.
[219] H. Furukawa, F. Gándara, Y.B. Zhang, J. Jiang, W.L. Queen, M.R. Hudson, O.M. Yaghi, Water adsorption in porous metal–organic frameworks and related materials, J. Am. Chem. Soc., 136 (2014) 4369–4381.
[220] S.S. Chui, S.M. Lo, J.P. Charmant, A.G. Orpen, I.D. Williams, A chemically functionalizable nanoporous material, Science, 283 (1999) 1148–1150.
[221] H. Xu, J. Gao, X. Qian, J. Wang, H. He, Y. Cui, Y. Yang, Z. Wang, G. Qian, Metal–organic framework nanosheets for fast-response and highly sensitive luminescent sensing of Fe^{3+}, J. Mater. Chem. A, 4 (2016) 10900–10905.
[222] S. Kumar, S. Jain, M. Nehra, N. Dilbaghi, G. Marrazza, K.-H. Kim, Green synthesis of metal–organic frameworks: a state-of-the-art review of potential environmental and medical applications, Coord. Chem. Rev., 420 (2020) 213407, doi: 10.1016/j.ccr.2020.213407.